Geologie und Paläontologie in Westfalen 99: 1–21 (2026)

GEOLOGIE UND PALÄONTOLOGIE IN WESTFALEN

LWL Für die Menschen. Für Westfalen-Lippe.

Two ornithodiran unguals from the Rhaetian bonebed of Warburg-Bonenburg (Germany): Possible evidence for dinosaurs and pterosaurs

Julia Hack[1]*, Darius Nau[1], Achim H. Schwermann[2] & P. Martin Sander[1,3]

[1] Bonn Institute of Organismic Biology, Section Paleontology, 53115 Bonn, Germany

[2] LWL-Museum für Naturkunde, Westfälisches Landesmuseum mit Planetarium, 48161 Münster, Germany

[3] School of Resources and Environmental Engineering, Hefei University of Technology, Hefei 230009, Anhui Province, China

* Corresponding Author: s6juhack@uni-bonn.de

Manuscript received 27.11.2024; accepted in revised form 28.07.2025

https://doi.org/10.64369/mkcm4334

Abstract. The clay pit of the Lücking Company near Warburg-Bonenburg (Höxter District, North Rhine-Westphalia, Germany) includes multiple bone beds within the Rhaetian Exter Formation. These provide records of a wide range of Late Triassic marine vertebrates. However, so far, a single tooth of a cynodont and a presumable sphenodont jaw fragment are the only terrestrial records among the fauna of otherwise marine and limnic affinity. Here we describe two unguals from Bone Bed 2 of this locality, which are not referable to any taxon previously identified from this fossil site. The larger of the two most closely resembles unguals of early-branching sauropodomorphs, especially *Plateosaurus* or *Massospondylus*. Although theropods cannot be fully excluded, we tentatively identify the smaller ungual as that of a pterosaur. This is suggested by morphological features, including the presence of sharp edges on the ventral margin, and by morphometric evidence. The described specimens represent the first record of either taxon for the locality of Bonenburg. Furthermore, they not only constitute one of the geologically youngest fossils of a non-sauropod sauropodomorph from Europe but also potentially the largest Triassic pterosaur.

Key words: Triassic, Sauropodomorpha, Pterosauria, Westphalia, Morphometrics

Kurzfassung. Die Tongrube der Firma Lücking bei Bonenburg (Kreis Höxter, Nordrhein-Westfalen, NW-Deutschland) umfasst mehrere Bonebeds innerhalb der rhätischen Exter-Formation. Diese liefern Belege einer breiten Spanne spät-triassischer, mariner Wirbeltiere. Bisher sind ein einzelner Zahn eines Cynodonten und ein Kieferfragment, vermutlich einer Brückenechse, die einzigen terrestrischen Funde neben der ansonsten marinen Fauna. Hier beschreiben wir zwei Ungualen des Bonebeds 2 dieser Lagerstätte, die keiner der dort bisher gefundenen Taxa zugeordnet werden können. Das größere der beiden ähnelt am meisten basalen Sauropodomorphen, insbesondere *Plateosaurus* und *Massospondylus*. Während Theropoden nicht vollständig ausgeschlossen werden können, identifizieren wir das kleinere Unguale vorsichtig als Pterosaurier, gestützt auf morphologische Merkmale einschließlich des Vorhandenseins scharfer Kanten am ventralen Rand, sowie auf morphometrische Belege. Die beschriebenen Exemplare sind die ersten Nachweise beider Taxa für den Fundort in Bonenburg. Darüber hinaus stellen diese nicht nur eines der geologisch jüngsten Fossilien eines nicht-sauropoden Sauropodomorphen aus Europa dar, sondern auch möglicherweise den größten triassischen Pterosaurier.

Schlüsselwörter: Trias, Sauropodomorpha, Pterosauria, Westfalen, Morphometrie

Introduction

Sauropodomorpha and Pterosauria are two pivotal clades that emerged during the Late Triassic, marking significant evolutionary advancements in terrestrial and aerial vertebrate life. Sauropodomorphs, herbivorous dinosaurs, exhibited a range of body sizes and locomotor adaptations, transitioning from bipedal to quadrupedal stances. Notable early sauropodomorphs include *Plateosaurus* from Europe and *Musankwa sanyatiensis* Barrett et al., 2024 from Zimbabwe, highlighting their widespread distribution across Pangaea. Their morphological diversity reflects adaptations to various ecological niches, contributing to their success during this period (Apaldetti et al. 2021; Barrett et al. 2024).

Pterosaurs, the earliest known vertebrates to achieve powered flight, also originated in the Late Triassic. Early representatives such as *Eudimorphodon*, *Preondactylus* and *Austriadactylus* from Europe demonstrate a variety of dental and skeletal adaptations, indicating diverse ecological roles and a broad geographic range. The emergence of these clades during the Late Triassic underscores a period of significant evolutionary innovation, with sauropodomorphs and pterosaurs occupying distinct but complementary niches in terrestrial and aerial ecosystems (Dalla Vecchia 2003; Eugénio Fernandes 2024).

The fossil locality of Bonenburg (Höxter District, North Rhine-Westphalia, Germany; Fig. 1) provides a diverse record of Triassic vertebrates (Sander et al. 2016, 2026; Schwermann et al. 2017). The finds come from clay pit #3 of the August Lücking brick factory, mostly from four bone beds within the Rhaetian Exter Formation (Gravendyck et al. 2020; Sander et al. 2026). The bone beds resemble similar and approximately coeval bone beds in the UK and France (Swift & Martill 1999; Allard et al. 2015; Sander et al. 2016, 2026; Slater et al. 2016; Cross et al. 2018). In addition to numerous chondrichthyan, actinopterygian, dipnoan (Sander et al. 2016, 2026) and rare actinistian (Hartung et al. 2021) fossils, the site has produced many notable finds of marine reptiles, including abundant material of Ichthyosauria (Perillo & Sander 2024; Sander et al. 2026), Plesiosauria (Wintrich et al. 2017) and the enigmatic *Pachystropheus*. *Pachystropheus* is traditionally regarded as the oldest known choristodere, but was more recently recovered as the youngest surviving thalattosaur (Quinn et al. 2024).

Non-marine and possibly marginally marine tetrapod finds consist of the youngest record of Phytosauria (Sander & Wellnitz 2024) and of non-brachyopoid Stereospondyli (Konietzko-Meier et al. 2019; Prino et al. 2024). The holotype of *Rhaeticosaurus mertensi* Wintrich et al., 2017, the oldest (and only Triassic) plesiosaur known from an articulated skeleton, was obtained in isolation from a location between bone beds 1 and 2 (Wintrich et al. 2017).

However, unequivocally terrestrial faunal elements from the Bonenburg bone beds have so far been limited to a single tooth of the cynodont *Lepagia gaumensis* Hahn et al., 1987 (Schwermann 2016) and a small jaw fragment with two teeth, which probably originates from a sphenodontan (Sander et al. 2016, 2026; Schwermann 2016).

The purpose of the present work is to describe two additional non-marine tetrapod taxa, represented by two amniote ungual phalanges, a small and a large one. The morphology of these specimens does not fit to any taxa previously identified from this locality. The large ungual belongs to a basal sauropodomorph dinosaur, the first dinosaur from the locality, and the small one probably to a pterosaur.

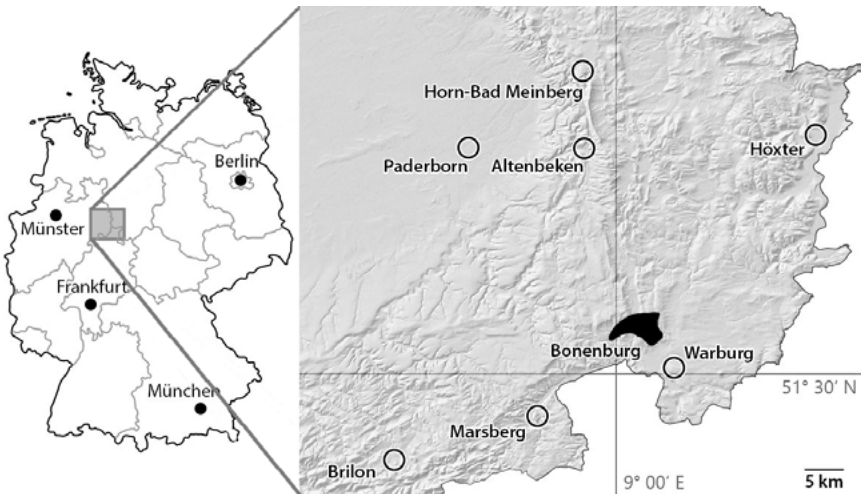

Figure 1: Locality of Bonenburg clay pit #3 of Lücking brick company in the eastern part of the state of North Rhine-Westphalia, Germany.

Materials and methods

Material studied

The two unguals studied were obtained as isolated fossils from Bone Bed 2 of the clay pit #3, located approximately 1 km north-west of the village of Bonenburg (North Rhine-Westphalia, Germany) and operated by the August Lücking brick company. Both specimens are housed in the palaeontological collection of the LWL-Museum für Naturkunde, Münster, Germany, under accession numbers WMNM P91001 and WMNM P19002.

Specimen WMNM P91001 was found by Michael Mertens (Altenbeken) in 2014, who reported it to the LWL-Museum für Naturkunde in Münster, where it was classified as a find falling under state ownership ("Schatzregal") according to § 18 of the North Rhine-Westphalia Monument Protection Act. Specimen WMNM P91002 was found during a palaeontological excavation by the University of Bonn in 2017. The two unguals are well-preserved and mostly unaffected by compaction. However, the distal tip as well as a part of the flexor tubercle of WMNM P91001 is missing, and there appears to be some amount of diagenetic collapse in the middle portions of both unguals.

For identification, morphological comparisons were made between these unguals and material from the collections of PIMUZ, SMF and SMNS, as well as various taxa from the literature.

Measurements

Dorsopalmar height of the unguals was measured at the highest point of the proximal articular surface. Proximodistal length was recorded in two ways: (1) as a straight-line measurement from the dorsoproximal tip of the extensor tubercle to the distal tip of the ungual, and (2) as a measurement orthogonal to the dorsopalmar height axis, representing the overall length independent of tubercle projection. All measurements were taken using digital calipers with a resolution of 0.01 mm and an accuracy of ±0.02 mm.

To quantify curvature, the unguals were positioned according to the orientation method described by Ostrom (1969), with the proximal articular facet aligned vertically in a straight, upright position. The radius of curvature was estimated by drawing a line from the inferred centre of rotation (approximated from the arc of the ventral margin) to the distal tip of the ungual. The curvature angle was then calculated between this radius and the dorsopalmar height axis.

Body size estimation

For all examined comparative taxa for which this information was available, the proportion of a linear metric of body size (total length or wingspan) to the length of their unguals was calculated. This proportion was then used to obtain size estimates for WMNM P91002 and P91001 on the basis of their measured ungual length, assuming isometric scaling.

To provide an approximate size estimate for WMNM P91002, assuming pterosaurian affinities, we performed an ordinary least squares (OLS) regression of log-transformed wingspan estimates and ungual lengths of the specimens listed in Table 1. Tested against an OLS regression fitted on the untransformed data, log-transformation eliminated heteroscedasticity and reduced the number and severity of potential outliers in the dataset (specimens with Cooks distances >4/n), at the expense of resulting in a non-normality of the residuals. In order to nevertheless provide robust confidence and prediction intervals, we performed a bootstrap with 1000 repetitions. For each repetition, the training data were randomly resampled, a new lm() model was fitted and predictions were generated from the model. For estimating prediction intervals, a randomly sampled residual of the respective model was added to the best-fit predictions. Quantiles across the 1000 repetitions were then used to generate the confidence and prediction intervals. Due to the limitations of this non-parametric approach, the precision of these intervals is limited and they are only reported to two significant digits.

Geometric morphometric analysis

As a quantitative test for the hypothesized systematic affinities of our specimens, a morphometric analysis of identified manual unguals (n = 76) pertaining to early (Triassic and Lower Jurassic) neotheropods (n = 22), pterosaurs (n = 12) and sauropodomorphs (n = 42) was conducted. Image material of the specimens was sourced from photographs or photogrammetric 3D models (DN, pers. obs., 2022; Christopher Griffin, Princeton, New Jersey, DN pers. comm., 2022) and published figures (Pterosauria: Wild 1978; Dalla Vecchia 2018, 2019, 2021; Sangster 2021; Sauropodomorpha: Young 1941; Pol & Powell 2007; Otero & Pol 2013; Barrett et al. 2019; Chapelle et al. 2019; Ballell et al. 2020; Nau et al. 2020; Schaeffer 2024 & DN, pers. obs., 2022; Theropoda: Huene 1934; Camp 1936; Colbert 1989; Nesbitt et al. 2009; You et al. 2014; Martill et al. 2016; Barta et al. 2018; Marsh & Rowe 2020; see also the electronic supplementary material S1).

Table 1: Size comparison of WMNM P91002 with Triassic and Lower Jurassic Pterosauria as well as two early Theropoda. Estimated wingspans/body lengths for WMNM P91002 are given based on the respective taxon and measurement/size estimation, broken down by the taxon used for scaling, as well as the respective measurements and size estimates.

Pterosauria

Taxon	Wingspan (m)	Ungual	Ungual length (mm)	Reference(s)	Wingspan estimate (m) for WMNM P91002
Carniadactylus	0.71	Pes	2.5	Dalla Vecchia (2009a)	7.2
			5.8		3.1
			5.9		3.1
			7.4		2.4
Dearc	2.04	Manus I	48.3	Jagielska et al. (2022)	1.1
		Manus II	41.4	Etienne et al. (2024)	1.3
		Manus III	36.6		1.4
Dimorphodon	1.5	Manus I	10	Sangster (2021)	3.8
		Manus I	12		3.2
		Manus II	16		2.4
		Manus II, III	18		2.1
		Pes I	9		4.2
		Pes I-IV	7		5.4
		Pes II-IV	8		4.8
Dorygnathus	0.97	Manus ?II	15.2	photogrammetric	1.6
		Manus ?I	11.5	measurements, Theda,	2.1
		?Manus	12.7	pers. comm. 2025	1.9
		Manus	14.3		1.7
		Manus	13.1		1.9
Eudimorphodon	0.75	Manus	6.5	Wild (1984)	2.9
			7.2		2.6
	1	Manus	6.5		3.9
			7.2		3.5

Theropoda

Taxon	Length (m)	Ungual	Ungual length (mm)	Reference(s)	Length estimate (m) for WMNM P91002
Tawa	2.3	Manus I	19	Nesbitt et al. (2009)	3.1
		Manus II	23		2.6
		Manus III	25		2.3
Panguraptor	2	Manus I	20	You et al. (2014)	2.4

In order to better account for the range of individual variation in ungual shape within species, multiple specimens were included, if available (particularly in the case of *Plateosaurus trossingensis* Fraas, 1913). This can potentially introduce biases towards classification in taxa represented by a higher number of specimens (i.e., Sauropodomorpha > Theropoda > Pterosauria) by widening their respective morphospaces. However, this was deemed acceptable for the purposes of the present work, since it effectively leads to a more stringent test of the proposed pterosaurian affinities for specimen WMNM P91002. The primary motivation for conducting the morphometric analysis was the uncertain taxonomic affinities of this specimen, and this approach avoids the loss of information about the morphometric variance within species that would result if each species were "flattened" into a single mean shape.

Ungual outlines (in pre- or postaxial view, used interchangeably) were traced in Inkscape (Inkscape Project 2020) and saved as black silhouettes on a white background. These silhouettes were then imported into R (version 4.4.0, R Core Team 2024), resampled to 1000

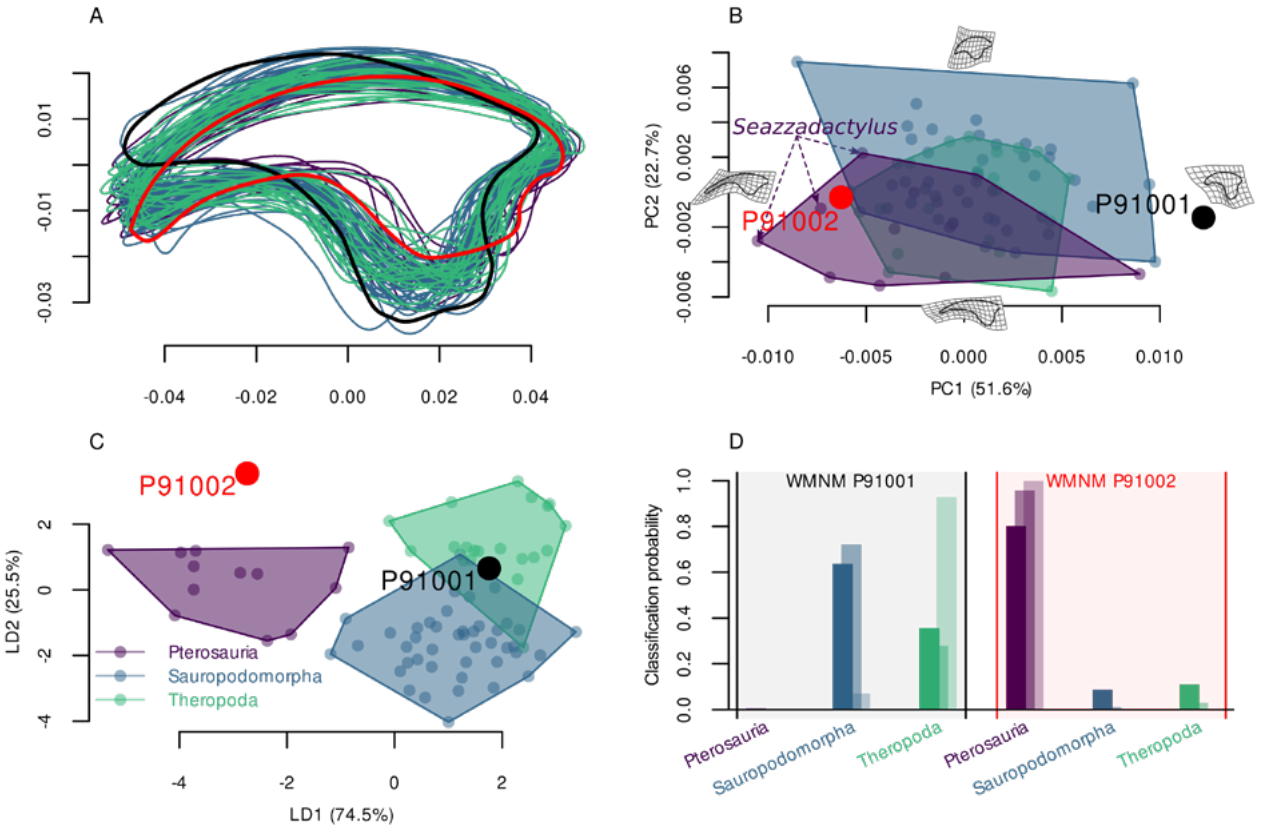

Figure 2: Results of morphometric analysis of ungual outline shapes. **A** Ungual silhouettes after tracing and alignment, as used as a basis for further analyses (WMNM P91001 and P91002 marked in black and red, respectively). **B** Results of principal component analysis on Fourier-transformed ungual silhouettes (entire dataset). **C** Results of linear discriminant analysis of scaled PCA results (note clear separation between Pterosauria and Dinosauria, but incomplete separation between Theropoda and Sauropodomorpha). **D** Taxonomic classifications made for WMNP P91001 and P91002 on the basis of the LDA (C). The three bars for each taxon and taxonomic grouping visualize the support measures (given as probabilities ranging from 0 to 1) for (from left to right): mean posterior probability based on a bootstrap with random taxonomic resampling (1000 repetitions), share of taxonomic classification in the respective group from among the bootstrap repetitions and the posterior probabilities in the full analysis (including all taxa exactly once).

outline points per specimen (R package "Momocs"; Bonhomme et al. 2014; Bonhomme & Claude 2022) and Procrustes-aligned (R package "geomorph"; Baken et al. 2021; Adams et al. 2022). The proximodorsal extremity of the claw (i.e., the dorsal "lip" of the articular facet, chosen because small portions of the claw tip are often missing) was treated as a fixed landmark and all other outline coordinates as sliding semi-landmarks (with Procrustes distance as the sliding criterium).

Aligned outline coordinates were then Fourier-transformed using the 12 harmonics ("efourier()" function of R package "Momocs"), after visually determining that these were sufficient to accurately capture the shape information in the outlines. The resulting Fourier coefficients were subjected to a principal component analysis (PCA), so that linear discriminant analysis (LDA; R package "MASS"; Venables & Ripley 2002, Ripley et al. 2022) was performed on the resulting (normalized) principal component scores, with the three taxonomic groups (Theropoda, Sauropodomorpha, Pterosauria) being used as factor levels for the response variable.

Specimens WMNM P91001 and P91002 were digitized, aligned and scaled together with the training data (all other specimens), but were removed from the sample and projected onto the PCA and LDA morphospaces for the remaining specimens to obtain classifications for the specimens relative to the material identified taxonomically. We assigned prior probabilities of one third to each of the three possible taxonomic groups before making predictions based on the LDA (thereby assuming equal prior probabilities for each group).

For validation, a sensitivity analysis with 1000 repetitions was run for the PCA and LDA analysis, with specimens randomly resampled (with replacement) from the entire outline dataset for each repetition. Two measures of bootstrap support were calculated, one as the proportion of repetitions resulting in the

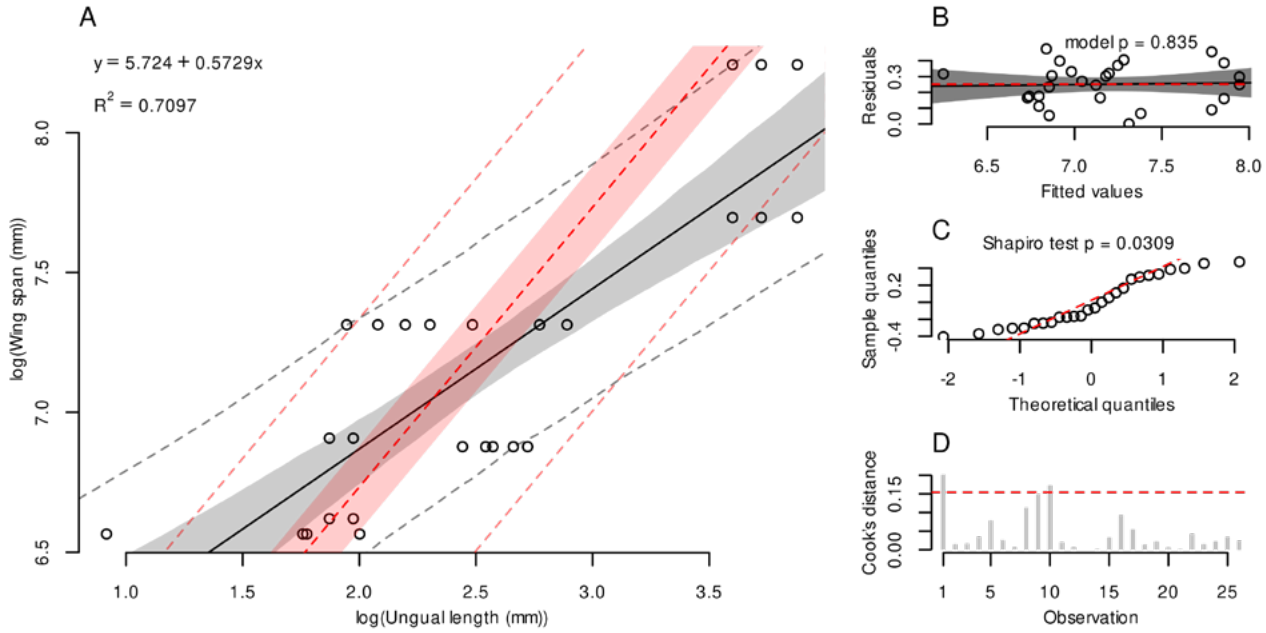

Figure 3: Estimation of body size for WMNM P91002 based on pterosaurs (Table 1). **A** model of log(wingspan)~log(claw length) (black/solid) compared to isometry (red/dashed), with respective bootstrap confidence (shaded polygon) and prediction (dashed margins) intervals. **B** Plot of absolute residuals against fitted values (showing no significant correlation, i.e., no heteroscedasticity). **C** Quantile-quantile plot of residuals (highlighting significant deviation from normality, p = 0.03).

respective taxonomic grouping as the most probable outcome, and another one as the mean of the posterior probabilities for each grouping across all bootstrap repetitions. All data and R code necessary for replication of this analysis are provided in the electronic supplementary material (S1).

Institutional abbreviations

GPIT, Institut und Museum für Geologie und Paläontologie, Universität Tübingen, Germany; MBR, Reptile collections, Museum für Naturkunde Berlin, Germany; MPUM, Museo Paleontologico del Dipartimento di Scienze della Terra, Università di Milano, Italy; PIMUZ, Paläontologisches Institut und Museum der Universität Zürich, Switzerland; SMNS, Staatliches Museum für Naturkunde Stuttgart, Germany; SMF, Sauriermuseum Frick; WMNM, LWL-Museum für Naturkunde Münster, Germany.

Results

Morphometric analysis

Principal components 1 and 2 explain approximately 75% of the variance. The PCA yielded poor separation between the morphospaces of the three taxa, with all three morphospaces overlapping considerably. When projected onto the PC1 × PC2 morphospace, WMNM P91001 plots outside any of the convex polygons of the taxonomic groups analysed, but closest to the basal sauropodomorphs *Plateosaurus trossingensis*, *Massospondylus carinatus* Owen, 1854 and *Schleitheimia schutzi* Rauhut et al., 2020. On the other hand, WMNM P91002 plots within the convex polygon of Pterosauria and outside (albeit close to) the convex polygons for Theropoda and Sauropodomorpha (Fig. 2B).

Linear discriminant analysis resulted in a good separation of the pterosaur morphospace from that of theropods and sauropodomorphs, but substantial overlap exists between the latter two groups (Fig. 2C). The results of the classification and the bootstrap-based sensitivity analysis for WMNM P91002 all support an assignment of the specimen to ?Pterosauria (full model posterior probability 99.9%, bootstrap support 95% in terms of share of classifications, 80% in terms of mean posterior probability). Conversely, full model LDA results for WMNM P91001 suggest a theropod classification for the specimen (posterior probability of 93%). However, a majority (72%) of the bootstrap repetitions instead support a sauropodomorph classification for the specimen, as does the mean posterior probability based on the bootstrap analysis (Sauropodomorpha: 64%, Theropoda: 36%).

Full results of the LDA classification for both specimens are presented in Table 2.

Table 2: Results of morphometric analysis. Mean posterior probabilities and share of classifications refer to the results of the bootstrap resampling, whereas the full model shows the estimated posterior probabilities from the baseline LDA run with each data point included exactly once.

	Pterosauria	Sauropodomorpha	Theropoda
WMNM P91001			
Mean posterior probabilities	0.0057	0.6373	0.3571
Share of classifications	0	0.721	0.279
Full model	0	0.0711	0.9289
WMNM P91002			
Mean posterior probabilities	0.8023	0.0869	0.1108
Share of classifications	0.958	0.012	0.03
Full model	0.9994	0	0.0006

Size estimation for WMNM P91001

The proportions in the virtually complete *Plateosaurus* skeleton GPIT1, as digitized by Mallison (2010), were used to provide an approximate estimate of body size for WMNM P91001. The total length of the skeleton GPIT1, as measured along the neural canal, is 5.57 m (Mallison 2010, fig. 10.2) and the articular lengths of the unguals of the first and second finger are 63 mm and 47 mm respectively (Mallison 2010, fig. 6), making them similar to WMNM P91001, where the same measurement is 59.95 mm. Assuming the same proportions between ungual length and total length as observed in GPIT1, total body length of WMNM P91001 can be estimated at 5.3 m and 7.1 m, based on the first and second digit, respectively.

Size estimate for WMNM P91002

Wingspan estimates based on our preferred identification of WMNM P91002 as a pterosaur were made based on both isometric scaling and a least squares regression model fitted to all data.

The Alpine Late Triassic pterosaur *Carniadactylus* has an estimated wingspan of 0.71 m and pedal unguals ranging from 2.5 mm to 7.4 mm (Dalla Vecchia 2009a). Simple scaling up would result in a wingspan estimate of about 2.4 m to 7.2 m for WMNM P91002. The wingspan of the Middle Jurassic pterosaur *Dearc* (Jagielska et al. 2022) was estimated by Etienne et al. (2024) to measure 2.04 m. Based on fig. 3A in Jagielska et al. (2022), the lengths of the manual unguals of *Dearc* are approx. 48.3 mm, 41.4 mm and 36.6 mm for digits I, II and III respectively. This would result in an estimated wingspan ranging from 1.1 m to 1.4 m for the Bonenburg specimen (Table 1).

The wingspan of an adult of the Early Jurassic *Dimorphodon* is estimated to be 1.5 m (Sangster 2021). Sangster (2021) described multiple individuals; to simplify the size comparison, the average lengths of the described unguals are used here. The unguals of manual digit I average 11 mm in length, those of digit II 17 mm and those of digit III 18 mm in length (Sangster 2021). The unguals of the first toe average 8 mm in length and those of the remaining toes average 7.5 mm each (Sangster 2021). The resulting ratios imply a wingspan of between 2.1 m and 5.1 m for WMNM P91002. *Eudimorphodon* has an estimated wingspan of 0.75 to 1 m (Stecher 2008). Figure 10 in Wild (1984) shows that the two preserved manual unguals are 6.5 mm and 7.2 mm long, resulting in wingspan estimates of 2.6–3.9 m for the Bonenburg ungual.

The OLS fit for the pooled data for manual and pedal unguals (Fig. 3A) results in a model that is highly significant ($p = 4.8E-07$) and explains 74% of the variance in wingspan. This model produces a mean estimated wingspan of 2.1 m for WMNM P91002, with a 90% confidence range of 1.8–2.3 m and a 90% prediction range of 1.1 m–3.0 m. The model fitted to only the manual unguals was also highly significant ($p = 1.4E-03$) and explains 71% of the variance in wingspan, with model parameters and results very close to the pooled model (mean wingspan estimate 2.1 m, 90% CI 1.7–2.3 m). The model fitted to only the pedal unguals produced a point estimate of 3.6 m (90% CI 1.0–6.1 m), but was not statistically significant ($p = 0.10$) due to insufficient sample size. It is therefore excluded from further consideration.

For an ungual length of 25.4 mm, our model for log(wingspan)~log(claw length) predicts a wingspan of 1.95 m (90% CI: 1.7–2.2 m, 90% PI: 1.3–3.1 m). This estimate is considerably lower than the isometric estimate derived from the mean proportions in

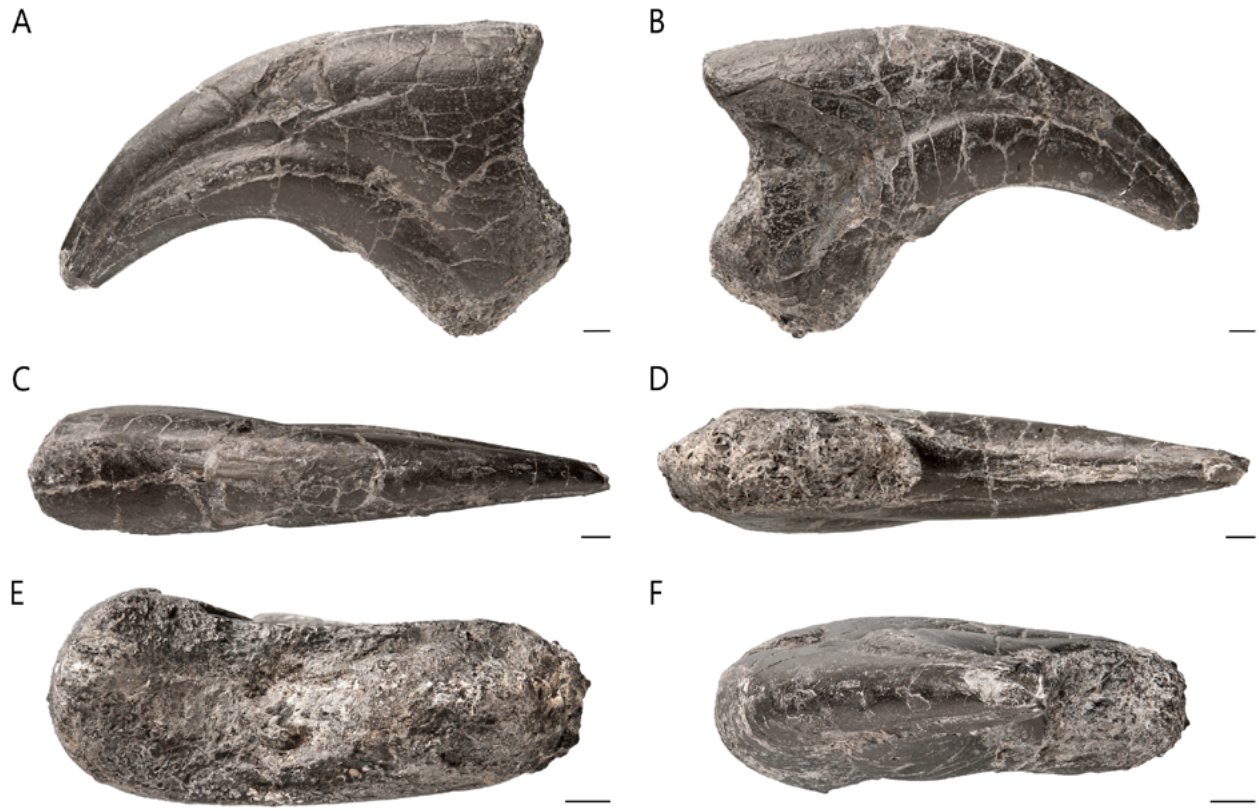

Figure 4: Large ungual (WMNM P91001) in all six views. **A** Left. **B** Right. **C** Dorsal. **D** Palmar; a shallow groove extends along the palmar surface. **E** Proximal (dorsal is to the left); the articular facet is poorly preserved. **F** Distal (dorsal is to the left). Scale bars represent 3 mm. Photos by Georg Oleschinski.

the sample, at 2.89 m (90% CI: 2.5–3.4 m, 90% PI: 1.4–5.3 m), highlighting the apparent negative allometry (exponent of 0.57) in the model.

If WMNM P91002 is, instead, treated as a theropod, its total length can be estimated on the basis of early-branching theropods (Table 1). *Panguraptor* from the Early Jurassic of China has a total length of approximately 2.0 m (You et al. 2014). The only fully visible ungual, that of the first digit, measures 2.0 cm (You et al. 2014). From the ratio of this ungual to the total length and the dimensions of the studied ungual, a total length of about 2.4 m is obtained for WMNM P91002.

Based on fig. 2 in Nesbitt et al. (2009), the total length of the early theropod *Tawa* is approximately 2.3 m. Likewise, the lengths of the terminal phalanges of the manus of this animal can be measured from a figure (Nesbitt et al. 2009, fig. 2F), and suggest that the ungual of the first digit measures 19 mm, that of the second digit measures 23 mm and that of the third digit 25 mm in length. These proportions imply total length estimates for WMNM P91002 of approximately 3.1 m, 2.6 m and 2.3 m, respectively.

Systematic palaeontology

Archosauria Cope, 1869
Ornithodira Gauthier, 1986
Dinosauria Owen, 1842
Sauropodomorpha Huene, 1932
Incertae sedis

Material examined. WMNM P91001; late middle Rhaetian Exter Formation, Contorta Beds, Bone Bed 2b, 20 m below the Triassic-Jurassic boundary (Gravendyck et al. 2020; Sander et al. 2026); clay pit #3 of the Lücking brick factory near Warburg-Bonenburg, Germany; 51°33‘47“N, 9°02‘16“E

Description. The length of the ungual, measured orthogonally to the height, is 59.5 mm, while the length from the distal tip to the dorsoproximal tip of the extensor tubercle is 62.4 mm. The dorsopalmar height of the ungual at the proximal end is 36.6 mm. The mediolateral width, measured at the widest point, is 13.8 mm. The angle between the height of the ungual and its radius is 77°.

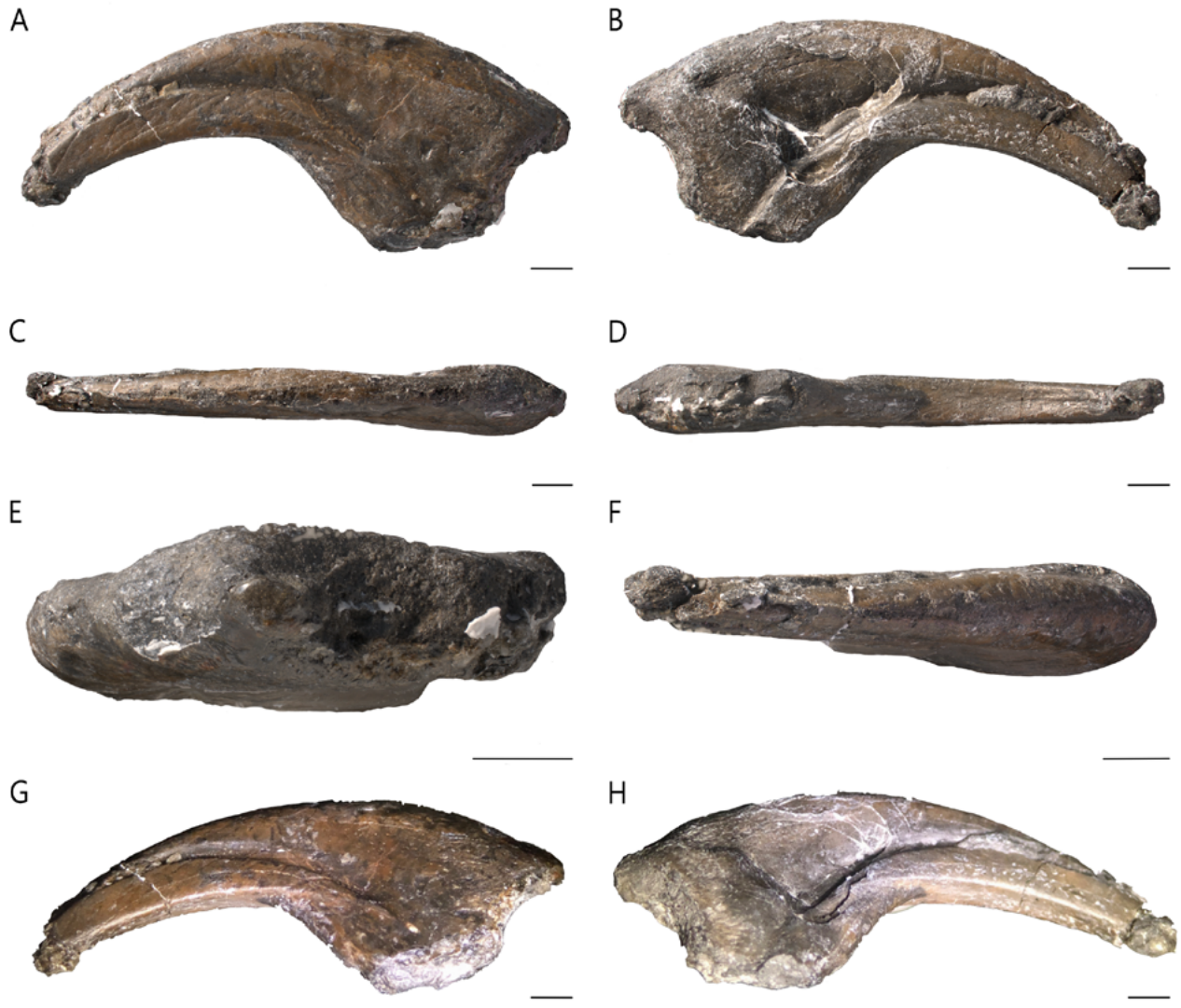

Figure 5: Small ungual (WMNM P91002) from all six sides (A-F). Sharp palmar margins of WMNM P91002 (G-H). **A** Left. **B** Right; this side shows taphonomic collapse. **C** Dorsal. **D** Palmar. **E** Proximal (left is dorsal). **F** Distal (left is dorsal). **G** Left side from slightly palmar view. **H** Right side from slightly palmar view. Scale bars represent 2 mm. Photos A-F by Georg Oleschinski; G-H by PMS.

The ungual is strongly curved. There is a lateral vascular groove up to 3 mm wide, extending parallel to the palmar margin from the middle of the flexor tubercle towards the distal tip. The claw displays a high degree of bilateral symmetry, although the lateral groove extends slightly more dorsally on the right side (Fig. 4B) compared to the left (Fig. 4A). Dorsal to the grooves, the ungual is narrower than palmar. The proximal side (Fig. 4E) bears a large (but partially eroded) flexor tubercle, which comprises almost two thirds of the dorsopalmar height. Dorsally of the flexor tubercle, there is a much smaller and pointed extensor tubercle. In the dorsal aspect (Fig. 4C), the ungual tapers strongly towards the distal tip. In cross section, this side is proximally mildly convex and distally strongly convex. The palmar side (Fig. 4D) is also convex in cross section, but this is less pronounced than on the dorsal side. A narrow, shallow groove extends centrally along the palmar surface of the ungual in a proximodistal direction.

Remarks. WMNM P91001 is best identified as a manus ungual ("thumb claw") of a basal sauropodomorph. The first and second unguals of the manus of basal sauropodomorphs are proximally much higher, mediolaterally flattened, more strongly curved and more symmetrical than those of the pes (Huene 1926; Young 1941; Galton & Kermack 2010; Otero & Pol 2013; Nau et al. 2020). It is therefore reasonable to assume that the ungual pertains to the manus, although we compared WMNM P91001 with pes unguals too.

The slight asymmetry with a slightly more dorsally positioned ridge on the lateral side (sensu Huene 1926,

i.e., the developmentally postaxial or anatomically ulnar side) suggests that WMNM P91001 corresponds to the right side of the body. However, this hypothesis is tentative due to the slight nature of this asymmetry.

Diapsida Osborn, 1903
Archosauria Cope, 1869
Ornithodira Gauthier, 1986
?Pterosauria Kaup, 1834
Incertae sedis

Material examined. WMNM P91002; late middle Rhaetian Exter Formation, Contorta Beds, Bone Bed 2b, 20 m below the Triassic-Jurassic boundary (Gravendyck et al. 2020; Sander et al. 2026); clay pit #3 of the Lücking brick factory near Warburg-Bonenburg, Germany; 51°33'47"N, 9°02'16"E

Description. The greatest length of the ungual is 25.4 mm (measured from the tip to the proximal end of the extensor tubercle), whereas the length measured orthogonally to the proximal height is 16.3 mm. The dorsopalmar height at the proximal end is 11.1 mm and the maximal mediolateral width is 3.5 mm. The angle between the height of the ungual and its radius is 49°.

The dorsal edge of the ungual is strongly curved, transcribing about one quarter of a circle. A shallow, longitudinal, uniformly curved vascular groove starts at the proximal margin, in the middle of the flexor tubercle. It then initially extends more palmarly before crossing into the dorsal half of the ungual just after the longitudinal midpoint of the ungual and terminates dorsally at the tip. Ventral to and confluent with the vascular groove, there are some impressions of blood vessels running in palmodistal direction. The ungual displays a high degree of bilateral symmetry. The left (Fig. 5A) and right sides (Fig. 5B) differ only slightly: the left side is more flattened overall, and the right side bears a deeper vascular groove. However, the right side shows some taphonomic collapse, which might be the cause of these differences.

The proximal end (Fig. 5E) of the ungual dorsally bears a very small, pointed extensor tubercle and a dorsopalmar high flexor tubercle, although the latter is more weakly developed than in WMNM P91001. A proximopalmar piece of the flexor tubercle appears to have broken off. The dorsal side of the ungual (Fig. 5C) is convex in cross section. The palmar side (Fig. 5D) is divided into two parts. The proximal one, which emerges from the flexor tubercle, is very narrow and uniformly convex, but it becomes less convex distally. Approximately 13 mm from the tip, the distal portion of the ungual tapers rapidly from the dorsopalmar deeper proximal portion, while the taper distal to this portion is more gradual both in dorsal/palmar and in preaxial/postaxial aspects. The distal part bears sharp, palmolateral edges that delimit a remarkably flat palmar surface (Fig. 5G, H). The sharp edges arise from the flexor tubercle and continue distally, paralleling the vascular grooves. The distal tip (Fig. 5F) of the ungual appears to be sharply pointed despite being slightly crushed and retaining a small piece of matrix.

Remarks. WMNM P91002 is a small (for a dinosaur) to large (for a Triassic pterosaur), strongly curved and transversely very narrow ungual with a prominent flexor tubercle. These are all morphological characteristics generally more typical of manual than pedal unguals, leading us to tentatively identify the claw as pertaining to the manus. Due to its high degree of symmetry, assignment to a specific body side remains unclear.

Discussion

Morphological comparisons and identification of WMNM P91001

The unguals of ornithischians (Galton 2014), pseudosuchians (i.e. *Ticinosuchus* PIMUZ T2817), silesaurids (Piechowski & Tałanda 2019), drepanosaurids (Renesto 1994), theropods (Huene 1934; Nesbitt et al. 2009; You et al. 2014; Marsh & Rowe 2020) and pterosaurs (Wild 1984; Dalla Vecchia 2009a; Dalla Vecchia 2021; Sangster 2021) all differ substantially in a combination of curvature and overall proportions. Furthermore Triassic members of these clades all appear to have unguals that are at most half the size of WMNM P91001, leading us to confidently reject a referral to any of these taxa.

The unguals of *Herrerasaurus ischigualastensis* Reig, 1963 are large and curved, but direct comparison (Novas 1993; Sereno 1993) shows that its manual unguals have a more angular flexor tubercle, a more strongly curved dorsal margin and a proportionally lower proximal end than WMNM P91001, while the pedal unguals are significantly straighter and do not have a prominent flexor tubercle (the general condition of dinosaurian pedal unguals).

The *Plateosaurus trossingensis* holotype, described by Schaeffer (2024), has a first manual ungual with an extensor tubercle that extends further proximally and a more strongly curved ventral margin than in WMNM P91001. The ungual of the second digit largely resembles WMNM P19001 in its overall shape, but its vascular groove ends dorsally of the tip while the groove seems to extend all the way to the tip in the Bonenburg specimen. The ungual of the third digit is much more gracile than WMNM P19001, less strongly curved and less high dorsoproximally.

The curvature of the dorsal margin of the manual unguals of the juvenile *Plateosaurus* SMF 15.8B. from Frick, Switzerland, is similar to that of WMNM P19001, while the curvature of the palmar margin increases from the first to the third digit (Nau et al. 2020).

Among all palmar margin curvatures, that of the first digit of SMF 15.8B. resembles the Bonenburg ungual the most. However, the first ungual of another, much larger *Plateosaurus* specimen from Frick (SMF 16.1.150, JH, pers. obs., 22.04.2022) has a proportionally taller proximal end and a stronger overall curvature. This trend is also seen when comparing WMNM P19001 to *Plateosaurus* SMF 20 and SMF 12.3.82 from Frick (JH, pers. obs., 22.04.2022). The ungual of a second digit of *Plateosaurus* SMF 11.4.7 shows a high degree of similarity to the Bonenburg specimen but bears an extensor tubercle which extends further proximally (JH, pers. obs., 22.04.2022). Based on these comparisons, WMNM P19001 most likely appears to derive from the first or second digit of the manus of a medium-sized basal sauropodomorph.

The entire manus of the small and basal *Thecodontosaurus antiquus* Riley & Stutchbury, 1836 is much more gracile than that of *Plateosaurus*, and the first manual ungual of *T. antiquus* is more strongly curved as well as more gracile than WMNM P91001 (Benton et al. 2000). On the other hand, the unguals of *Pantydraco caducus* Galton et al., 2007 are less curved (Galton & Kermack 2010) than WMNM P91001. While Galton (1973) does not describe the unguals of *Efraasia diagnostica* Huene, 1908, the included figures show that they are straighter, have a smaller flexor tubercle, and their extensor tubercle extends further proximally than in the Bonenburg ungual. Based on the description by Otero & Pol (2013) of the unguals of *Mussaurus patagonicus* Bonaparte & Vince, 1979, its first digit ungual is less curved and has a more proximally extending flexor tubercle than WMNM P91001; furthermore, the medial groove is more curved than the lateral one, whereas the grooves in WMNM P91001 have the same curvature. The ungual of the second manus digit is less curved, smaller and less high than the Bonenburg ungual and differs in the pathway of the grooves. Only the unguals of the pes were described for *Riojasaurus incertus* Bonaparte, 1969 (Van Heerden & Galton 1997), so this taxon cannot be excluded from consideration. The same is the case for *Blikanasaurus cromptoni* Galton & Van Heerden, 1985 (Galton & Van Heerden 1998) and *Aardonyx celestae* Yates et al., 2010.

Based on figures in Young (1941), it is clear that the unguals of the second and third digits of *Lufengosaurus huenei* Young, 1941 have less prominent flexor tubercles, a less dorsoventrally tall proximal end and are, especially in the distal portion, much less curved than in the Bonenburg specimen. The first ungual, on the other hand, bears greater resemblance to WMNM P91001, although it is distally more strongly curved. The first digital ungual of *Massospondylus carinatus* also closely resembles the Bonenburg ungual. However, it is more curved and the vascular grooves begin just dorsal of the flexor tubercle (Barrett et al. 2019) while they continue along the midline of the flexor tubercle in WMNM P91001. The unguals of the second and third digits are much shorter, more slender, less tall dorsopalmarly and less curved than both the first digit ungual (Barrett et al. 2019) and the Bonenburg specimen.

Rauhut et al. (2020) mentioned only a single pedal ungual of *Schleitheimia schutzi*. However, examination of the material at the PIMUZ revealed a presumed manual ungual on display (PIMUZ A/III 1546), which is described and compared to WMNM P91001 here. The specimen bears deep vascular grooves on both the medial and lateral surfaces. These start on the proximal end above the flexor tubercle and run between the midline and the dorsal margin, parallel to the palmar margin, up to the distal tip. WMNM P91001 has similar grooves, however they start at the midline of the flexor tubercle and extend along or only slightly above the midline of the ungual. In *Schleitheimia*, the ungual is slightly widened dorsal to the grooves and more strongly widened palmar to them. This causes the proximal side to be much wider palmarly than dorsally. In the Bonenburg ungual, however, the dorsal portion of the proximal side is slightly wider than the palmar one. Both unguals have a pointed, proximodorsal extensor tubercle and a large, rounded, proximopalmar flexor tubercle. The ungual of *Schleitheimia* has considerably less curvature than WMNM P91001.

In conclusion, WMNM P91001 can confidently be identified as a manual ungual of an early-branching

sauropodomorph based on its robust construction, pronounced flexor tubercle and strong curvature—features typical of the first or second manual digits in this group. The ungual shows notable morphological similarity to unguals of *Plateosaurus*, particularly juvenile individuals such as SMF 15.8B. from Frick, Switzerland (Nau et al. 2020), in which the curvature of the dorsal and palmar margins closely matches that of the Bonenburg specimen. This resemblance is especially marked in the ungual of the first digit, though variation among individuals and ontogenetic stages is evident in the Frick assemblage. Comparisons with *Massospondylus carinatus* further support this identification, as its first manual ungual shares key features with WMNM P91001, including overall shape and robustness, though minor differences exist in the course of the vascular grooves (Barrett et al. 2019). Given the abundance of *Plateosaurus* material from the Late Triassic of Central Europe and the likely presence of massospondylids or related massopodans in the European Triassic (Regalado Fernandez & Werneburg 2022; Alessandro Lania, DN pers. comm., 2024), this assignment is both well-supported and stratigraphically plausible.

Morphometric analysis of WMNM P91001. Our analysis yielded an ambiguous result for WMNM P91001. In PCA morphospace, no clear taxonomic signal could be determined. This is not unexpected, due to the unguided nature of the PCA, which seeks to determine axes of greatest variance irrespective of their taxonomic signal. Unsurprisingly, LDA yielded a considerably better separation between groups, with pterosaurian morphospace fully separated from that of dinosaurs and theropods, while the theropod and sauropodomorph morphospaces retained a substantial, albeit greatly reduced, overlap. Although the full model run of the LDA (full taxon inclusion) classifies WMNM P91001 as a probable theropod (93% posterior probability and within the convex hull for this clade), it is located very close to this overlapping region in the morphospace (Fig. 2C). The sensitivity analysis, however, suggests a more probable identity as a sauropodomorph (72% of bootstrap repetitions supporting a sauropodomorph identity vs 28% supporting a theropod identity, with a mean posterior probability of 64% for a sauropodomorph identity vs 36% for a theropod identity; Table 2), which is also more in line with our morphological assessment of the specimen. This discrepancy between the full sample and the sensitivity analysis implies that our morphometric approach is too sensitive to random effects of taxonomic sampling to reliably distinguish theropod from sauropodomorph unguals, so the result from the full sample is apparently non-representative when the effects of random taxonomic sampling are considered.

There is, however, a tendency (from the sensitivity analysis, which is less affected by such biases due to the random resampling employed across the dataset) to support our morphological assignment of the specimen to Sauropodomorpha. As discussed above, a theropod identity for WMNM P91002 appears highly unlikely on the grounds of size and robusticity (the latter even when comparing theropods to small or juvenile sauropodomorph unguals, such as those of SMF 15.8B.), while a sauropodomorph identity is highly probable on these grounds. We therefore suggest that this identification is likely the correct one, and also highlight the need for careful consideration of the effects of taxonomic sampling for morphometric discriminant analyses in general.

Limitations of the morphometric methodology employed include the restriction to a single, uninterrupted outline per ungual, which reflects the underlying limitations of the elliptical Fourier transformation used to quantify ungual shape. Previous analyses of ungual morphometrics have mostly relied on traditional (non-geometric) measurement-based approaches (e.g., Tinius & Russell 2017; Thomson & Motani 2021). This was, however, deemed infeasible for our specimens, due to the frequent lack of 3D-preservation of comparative material (in particular that of pterosaurs) and the resulting unavailability of three-dimensional measurements. Other analyses employed a limited number of fixed landmarks (e.g., Hedrick et al. 2019) and/or relied heavily on sliding semi-landmarks to quantify parts of the unguals that do not contain homologous points on which fixed landmarks could be placed (e.g., D'Amore et al. 2018). Our own approach, using elliptical Fourier transformation of the ungual outlines, avoids these issues and allows quantification of the entire outline shape (for a similar analysis, see Lautenschlager 2014).

However, some aspects of ungual morphology could not be captured using this technique. This especially applies to the shape of the vascular grooves, as these are separate features outside of the closed outline shape used as a basis for the Fourier transformation. Development of a technique to incorporate this additional information into an outline-based morphometric analysis would thus represent an interesting avenue for future research and might enable better discrimination between different groups of dinosaurian unguals.

Body size estimate of WMNM P91001. The specimen WMNM P91001 falls within the size range of manual unguals known from basal sauropodomorphs, including the European *Plateosaurus* (e.g., Schaeffer 2024; JH and DN, pers. obs., 2022). Both body size estimates calculated here for WMNM P91001, at 5.29 m and 7.08 m, are also well within the body size range reported for *Plateosaurus* (Sander 1992; Sander & Klein 2005; Mallison 2010; Nau et al. 2020). More broadly, the lengths of other reported manual unguals in basal Sauropodomorpha (*Plateosaurus*: Schaeffer 2024; Huene 1926; DN, pers. obs., 2020 and 2022; *Massospondylus*: Barrett et al. 2019; *Mussaurus*: Otero & Pol 2013; *Thecodontosaurus*: Benton et al. 2000; *Efraasia*: Galton 1973; *Lufengosaurus*: Young 1941) ranges from 50 mm to 110 mm, with the exception of the early-stage *Plateosaurus* juvenile SMF 15.8B. (Nau et al. 2020) and *Pantydraco* (Galton & Kermack 2010). With a length of 62.4 mm, the Bonenburg ungual is therefore within the typical size range of mid-sized basal sauropodomorphs.

Morphological comparisons and identification of WMNM P91002

Assuming WMNM P91002 has theropod affinities, the unguals of sauropodomorphs are much larger and more robust, those of silesaurids (Piechowski & Tałanda 2019) are also much more robust and those of drepanosaurids (Renesto 1994) are shorter and broader than the Bonenburg ungual. While ontogenetic variation in ungual morphology is not well studied in non-avian dinosaurs or extant animals (Birn-Jeffery et al. 2012), the unguals of the juvenile *Plateosaurus* specimen (SMF 15.8B.) are also much larger and more robust than WMNM P91002. These groups can therefore be confidently excluded, leaving other archosauriforms as the most likely remaining possibilities for the taxonomic identity of the specimen.

Among pseudosuchians, pedal unguals of the "rauisuchian" *Ticinosuchus ferox* Krebs, 1965 (PIMUZ T 2817) are short, slightly curved and have a small, rounded flexor tubercle as well as longitudinal grooves running parallel to the dorsal margin. The distal part of the unguals (apart from the distal-most part) is only marginally thinner in dorsoplantar direction than the proximal end, differing markedly from WMNM P91002. Therefore, their entire form does not resemble the Bonenburg ungual, and *Ticinosuchus* or similar pedal unguals can be confidently excluded. The claws of the manus are very small and almost triangular, with a barely curved palmar side and a strongly curved dorsal margin. The proximal end is much taller in dorsopalmar diameter than the distal end and bears a small flexor tubercle. Here too, the shape of the unguals does not resemble WMNM P91002, which has a proximal portion expanded in dorsopalmar direction and a gracile, heavily tapered and curved distal part.

Basal ornithischians can be confidently excluded as well due to their subconical, short claws, which are neither curved nor possess prominent flexor tubercles (Galton 2014). *Heterodontosaurus tucki* Crompton & Charig, 1962 is an exception to this generalisation as its unguals are curved and have a flexor tubercle (Galton 2014). However, the longitudinal grooves do not end dorsally of the distal tip (Sereno 2012) like those in WMNM P91002, and the claws of *Heterodontosaurus* are more deeply curved.

Since the smaller Bonenburg ungual bears similarities to theropod unguals due to its transversally flattened and strongly curved form ending in a sharp tip, here it is compared with the claws of some basal theropods. The claws of *Herrerasaurus ischigualastensis* (although it may fall outside of Theropoda) are more robust and have more strongly curved vascular grooves which do not end dorsally of the distal tip (Sereno 1993). Within Theropoda, sharp edges or keels on the palmar side of the manual unguals appear to have been described only for members of Maniraptora (e.g., Novas et al. 2005).

Based on the illustration of the manus of *Tawa hallae* Nesbitt et al., 2009 in Nesbitt et al. (2009), the ungual of the second digit most closely resembles WMNM P91002 in its elongated and curved shape. Unfortunately, it is not clear from the figure or description whether the palmar side is flattened and shows sharp edges or not. It is, however, more likely that there are no sharp edges present, as *Panguraptor* and *Dracoraptor* are the only coelophysoids examined here which seem to exhibit such sharp margins, based on the figure in You et al. (2014). While Zahner & Brinkmann (2019) do not describe the unguals of *Notatesseraeraptor frickensis* Zahner & Brinkmann, 2019 in detail, personal observations (JH, 22.04.2022) of the holotype and only specimen (SMF 06-1) allow comparisons. The manual claws of *N. frickensis* are curved and much deeper proximally than distally. The lateral longitudinal groove is shallow and extends along the midline of the claw. The proximal end bears a slightly rounded dorsal extensor tubercle and a large, pointed, ventral flexor tubercle, differing from the morphology of WMNM P91002. The claws of *Dilophosaurus wetherilli* Welles, 1970 (Marsh & Rowe 2020) are much more robust than WMNM P91002 and have less prominent

longitudinal grooves. Those of *Liliensternus liliensterni* Welles, 1984 (Huene 1934) are only incompletely preserved, but are likewise far more robust (much deeper dorsoventrally) than the Bonenburg ungual. Furthermore, the articulation facet in *L. liliensterni* is divided, and about a third of the total height lies below the division (Huene 1934). In WMNM P91002, on the other hand, about three quarters of the total height lies below the division of the articulation facet.

Camp (1936) assigned two claws to the manus of *Segisaurus halli* Camp, 1936, which he figured but did not describe in detail. Carrano et al. (2005) described them as thin and strongly curved, much like the ungual examined here. However, based on the figure in Camp (1936), it is clear that the vascular grooves differ in shape, and it is unfortunately not possible to determine whether the claws have sharp palmar edges or a palmar keel. The first manual ungual of *Panguraptor lufengensis* You et al., 2014 (You et al. 2014) strongly resembles the Bonenburg ungual in its slim, strongly curved shape with a large flexor tubercle and an apparent sharp edge on the palmar margin of at least one side. Unfortunately, You et al. (2014) do not describe the unguals of *Panguraptor*, so our assessment is purely based on the illustration, in which the unguals are partially obscured. While the unguals of *Coelophysis bauri* Cope, 1889 are also thin and strongly curved (Colbert 1989), they are mediolaterally broader, dorsoventrally deeper and proximodistally shorter than WMNM P91002. The *Coelophysis* unguals depicted in Barta et al. (2018) are more gracile than the ones figured in Colbert (1989) but are less curved than the Bonenburg specimen. While the first digit manual ungual of *Dracoraptor hanigani* Martill et al., 2016 is much more robust than WMNM P19002, and manual ungual III is much less curved, the ungual of digit II does bear some resemblance. Unfortunately, it is largely obscured by the matrix and associated bones. However, the curvature is similar to WMNM P19002. It also appears to bear a sharp ventral margin (Martill et al. 2016). The unguals of *Coelophysis (=Syntarsus) rhodesiensis* Raath, 1969 (Galton 1971; Barta et al. 2018; Christopher Griffin, DN pers. comm., 2022) are shorter and more robust than WMNM P91002, even though Galton (1971) describes them as transversally flattened and sharp.

Turning to pterosaurs, Dalla Vecchia (2009b) does not describe the manual unguals of *Austriadactylus cristatus* Dalla Vecchia et al., 2002, which are obscured by the skull in the figure, so their similarity to the Bonenburg ungual cannot be determined. The holotype of *Austriadraco dallavecchiai* Kellner, 2015 includes a 6.7 mm long manual ungual (Dalla Vecchia 2021). While it seems to show a sharp edge on the palmar margin, the shape of the ungual differs from WMNM P91002 in the different degrees of curvature of the dorsal and palmar margins and a longer distal part of the claw in *Austriadraco*. The claws of the second and third manual digit of *Seazzadactylus venieri* Dalla Vecchia, 2019 also have a more elongate distal part than WMNM P91002 and a less curved dorsal margin (Dalla Vecchia 2019). The first digit manual ungual of *Seazzadactylus* strongly resembles the Bonenburg ungual in its overall shape, proportions and curvature, merely the proximal end is dorsopalmarly higher than in WMNM P91002. Only two incomplete unguals of the manus are preserved of *Carniadactylus rosenfeldi* Dalla Vecchia, 1995 (Dalla Vecchia 2009a). These are described as larger than the pedal unguals, robust (for a pterosaur), elongated, slightly curved and similar to those of *Dimorphodon* (Dalla Vecchia 2009a). This description does not really fit WMNM P91002, but since the manual unguals (unlike their pedal counterparts) are not well visible in any of the figures, comparisons are limited. The indeterminate manual ungual figured by Dalla Vecchia (2009a, fig. 2) appears to be more robust than the Bonenburg specimen, but the incompletely visible manual ungual III (Dalla Vecchia 2009a, fig. 5) seems to have a more gracile distal portion by comparison. However, in another specimen of *Carniadactylus* (MPUM 6009, originally described as "*Bergamodactylus*" Dalla Vecchia 2018), two manual unguals are preserved (Dalla Vecchia 2018, fig. 2). These indeed appear more robust and dorsoventrally taller than WMNM P91002.

For *Raeticodactylus filisurensis* Stecher, 2008, illustrations in Stecher (2008) show a single manual ungual that resembles WMNM P91002 in its overall shape, but the low resolution of the figure precludes more detailed comparisons. Only one photo of a single pedal ungual of *Peteinosaurus zambelli* Wild, 1978 has been published (Dalla Vecchia 2003). It is proximally much deeper than the Bonenburg claw and has a less strongly curved dorsal margin. The position and shape of the longitudinal grooves, however, are quite similar.

Based on the photos provided in Sangster (2021), it is evident that the unguals of the second and third finger of *Dimorphodon macronyx* Buckland, 1829 are more gracile and less curved than WMNM P91002. The ungual of the first digit, on the other hand, matches the Bonenburg ungual in its general shape, although the longitudinal groove extends along the midline in *Dimorphodon* and not dorsal of the midline, as in WMNM P91002. Wild (1984) mostly focuses on the

function of the unguals of *Eudimorphodon ranzii* Zambelli, 1973 and less on their form, but his illustrations of two manual unguals show them to resemble the Bonenburg ungual in terms of curvature. The *Eudimorphodon* unguals are more robust overall, however, and dorsoventrally deeper, with a shorter distal portion of the claw. The manual unguals of *Dorygnathus banthensis* Theodori, 1830 are very long, gracile and sharp, much like WMNM P91002 (observed in specimen MBR 3665.1). The vascular groove does not extend dorsally of the distal tip in *Dorygnathus* (except in one disarticulated ?manual ungual). However, the unguals do appear to share the same flat palmar surface as WMNM P91002, although the delimiting keels are not as acute as in the latter (Denis Theda, DN, pers. comm., 2025). The palmar side is flattened and bears a sharp edge at least on one side (while the other is hidden in the matrix, Alessandro Lania, DN pers. comm., 2022), similar to the Bonenburg specimen. The manual unguals of *Dearc sgiathanach* Jagielska et al., 2022 are illustrated in Jagielska et al. (2022). The first digit claw of the manus has a much stronger curvature, the second digit has a more strongly curved palmar margin and the third digit is less curved than WMNM P91002. Furthermore, the longitudinal groove extends along the midline of the claws, whereas it runs above the midline in WMNM P91002. Two of the ?manual claws of *Rhamphorhynchus longicaudus* Meyer, 1847 are slightly more curved and have a shorter distal portion than WMNM P91002. The third one, however, while still a bit more curved and slightly shorter, resembles the Bonenburg claw in its overall shape.

While WMNM P91002 exhibits strong curvature, a narrow transverse profile and a prominent flexor tubercle—features typically associated with manual unguals in ornithodirans—we note that pedal unguals in non-pterodactyloid pterosaurs can also show similar morphology. Notable examples include *Dimorphodon macronyx*, *Jeholopterus ninchengensis* Wang et al., 2002, *Carniadactylus rosenfeldi*, and various rhamphorhynchines and darwinopterans such as *Dorygnathus banthensis*, *Changchengopterus pani* Lü, 2009, *Darwinopterus modularis* Lü et al., 2010, *Kunpengopterus sinensis* Wang et al., 2010, *Wukongopterus lii* Wang et al., 2009 and *Jianchangopterus zhaoianus* Lü & Bo, 2011, in which pedal claws exhibit well-developed flexor tubercles and strong curvature (Lü et al. 2010; Witton 2013). Nevertheless, pedal unguals in pterosaurs are generally smaller and slenderer than their manual counterparts, particularly in digit V, and their size is constrained by functional limitations related to terrestrial locomotion and perching (Padian 1983; Unwin 1996). Given the relatively large size of WMNM P91002, identifying it as a pedal element would imply an unusually large and morphologically atypical pes for a Triassic pterosaur, resulting in implausibly high body size estimates (see Table 1). Therefore, although we acknowledge these exceptions and stress the need for caution, the combination of size, robust morphology and comparative outline analysis suggests a tentative identification as a manual ungual to be the most parsimonious.

Morphometric analysis of WMNM P91002. As with WMNM P91001, the PCA results alone proved insufficient to unambiguously classify this specimen. While WMNM P91002 falls only within the pterosaurian convex polygon in PC1 × PC2 morphospace, it plots extremely close to the convex polygons of the other two taxa (Fig. 2B), suggesting that a reliable taxonomic identification cannot be made based on the PCA alone. However, a sufficient separation of the pterosaurian from the dinosaurian morphospace could be achieved in the LDA (Fig. 2C). Based on the LDA run on the full sample, the posterior probability for a pterosaurian classification for WMNM P91002 is estimated at 99%. Support for this classification remained consistently high in the sensitivity analysis (96% of preferred classifications and 80% mean posterior probability for a pterosaurian classification across 1000 bootstrap repetitions). These results suggest that this inference (in contrast to that for WMNM P91001) and the morphometric separation between pterosaurian and dinosaurian unguals in our dataset is robust to the taxonomic sampling in the training data and sufficient as corroborating evidence for our favoured taxonomic identification of the specimen as a pterosaur on morphological grounds. For further discussion of the limitations of the morphometric analysis presented here, and the possibility for future expansion, see discussion on WMNP P91001 above.

Among pterosaurs, WMNM P91002 appears to plot closest to *Seazzadactylus* in PC-morphospace (Fig. 2B), although we do not consider a genus-level identification of the specimen feasible (or reasonable) considering the extremely incomplete state of the remains.

Body size estimate of WMNM P91002. Based on the proportions seen in the theropod *Panguraptor*, the estimated body length of WMNM P91002 is 2.4 m, which is only slightly above the body length of *Panguraptor* and *Tawa*. The estimate based on the proportions of *Tawa* is somewhat higher, at 2.3–3.1 m, but is still well

within the typical size range of Triassic theropods (e.g., comparable to *Tawa* itself).

When treated as a pterosaur, wingspan estimates using manual unguals for scaling ranged from 1.1–3.9 m, while estimates using pedal unguals for scaling ranged from 2.4–7.2 m. Even though a wingspan of 3.9 m is much larger than any known Triassic pterosaur, the even larger estimates based on pedal unguals suggest that WMNM P91002, assuming pterosaur affinities, belongs to the manus.

We acknowledge the inherent unreliability of size predictions based on isolated unguals as well as the limitations of our relatively small dataset of ungual and body size data. Hence, our size estimates (including those based on the presumed pterosaurian identity of WMNM P91002) should not be viewed as providing a reliable body size for the specimen, but only as roughly indicative.

Nonetheless, based on both the wingspan estimates and a direct comparison of ungual sizes, WMNM P91002 would appear to be large compared to other Triassic pterosaurs, whose wingspans do not exceed 1 m, at maximum ungual lengths of less than 1 cm (Table 1). Even the lower bound of our prediction band for wingspan, at 1.1 m, would be very large for a Triassic pterosaur, although it is well within the size range reached by some Lower Jurassic Pterosaurs (e.g., *Dimorphodon*; Sangster 2021). Our best-fit estimate approaches 2 m, which would put WMNM P91002 well in excess of the size range of any other known Triassic pterosaur. Size estimates based on direct, isometric scaling from the proportions in our comparative sample also tended to be higher than those based on the OLS regression model, with a predicted value of 2.89 m and a 90% prediction band ranging from 1.4–5.3 m. However, the upper half of this range should be viewed with great caution due to the negative allometry of wingspan with respect to ungual sizes in the OLS model, and since it would imply larger sizes than Jurassic pterosaurs (*Dearc*) that had larger unguals than WMNM P91002.

Implications for the Bonenburg fauna

The two unguals reported here represent the first ornithodiran remains from the Bonenburg claypit (compare for example Sander et al. 2016, 2026). This is surprising, given that no ornithodiran teeth (nor any other remains referable to the group) have been identified from the locality so far, even though they might be expected to be more common than bones. As such teeth can be expected to be quite small and inconspicuous, this highlights a need for continued careful examination of the numerous small dental elements present in the Bonenburg bone beds to prevent misidentification of possible reptilian teeth (for example as those of the very common *Saurichthys*, see Sander et al. 2016, 2026). On the other hand, the situation with the ornithodiran unguals parallels that of the phytosaur remains. The clade is only represented by a single osteoderm, and phytosaur teeth are conspicuously absent (see discussion in Sander & Wellnitz 2024; Sander et al. 2026).

Furthermore, the larger of the two unguals represents one of the youngest European fossils of non-sauropod sauropodomorphs, filling a regional stratigraphic gap in the fossil record of the group at least for continental Europe (see Galton & Upchurch 2004). The smaller ungual most likely represents a pterosaur, the first reported from the locality of Bonenburg. If this identification is correct, it would also make it probably the largest pterosaur known from the Triassic. Finally, the two unguals represent only the third and fourth reported cases of a clearly terrestrial faunal component from the locality, with the only previous record being a single tooth of the cynodont *Lepagia gaumensis* (Schwermann 2016) and the presumed jaw fragment of a sphenodontan (Sander et al. 2016, 2026), although we note that the occurrence of a pterosaur is not a strong indicator of terrestrial fossil input at the locality, since almost all Triassic pterosaurs are known from marine deposits.

Conclusions

Based on its large size, robust build, strong overall curvature and the prominent development of the flexor tubercle, WMNM P91001 can be confidently referred to an early-branching sauropodomorph. Its morphology closely matches that of the first manual unguals of plateosaurids and massospondylids, especially *Plateosaurus* (e.g., SMF 15.8B; Nau et al. 2020) and *Massospondylus carinatus* (Barrett et al. 2019). The Bonenburg specimen falls well within the morphological variation observed in these taxa, particularly in terms of digit-specific shape, dorsopalmar height and curvature, supporting referral to the first or possibly second manual digit of a non-sauropod sauropodomorph.

The smaller ungual, WMNM P91002, is more difficult to classify definitively, but its morphology aligns most closely with that of early-diverging pterosaurs such

as *Seazzadactylus* and *Austriadraco* (Dalla Vecchia 2019, 2021). Its moderately curved dorsal margin, elongate shape and the sharp-edged, flattened palmar surface—commonly observed in pterosaur manual unguals—collectively suggest pterosaurian affinities. Notably, its size exceeds that of any currently known Triassic pterosaur unguals, which may reflect either allometric scaling or taxonomic diversity not yet captured in the fossil record. This interpretation is further supported by our geometric morphometric analysis, which places WMNM P91002 within the pterosaur morphospace with high statistical confidence. Nonetheless, some caution is warranted: a theropod identity cannot be entirely excluded, as certain manual unguals of *Tawa*, *Panguraptor* and *Segisaurus* show overlapping characteristics, including sharp ventral ridges that also appear in some coelurosaurs (e.g., *Dracoraptor*). However, the overall morphology of WMNM P91002 appears more consistent with early pterosaurs than with theropod dinosaurs.

Data availability statement

Supplementary material S1: Supplementary data for morphometric analysis with R code, silhouette image files and landmark sets: Hack, J., Nau, D., Schwermann, A.H. & Sander, M.P. 2026: Data from: Two ornithodiran unguals from the Rhaetian bonebed of Warburg-Bonenburg (Germany): Possible evidence for dinosaurs and pterosaurs. – Zenodo. https://doi.org/10.5281/zenodo.19238381

Acknowledgements

We thank Alessandro Lania (Museo di Storia Naturale di Milano) and Denis Theda (Lippisches Landesmuseum Detmold) for invaluable discussions regarding the identity of the smaller specimen, as well as for providing specimen photographs and first-hand observations. We further want to thank Torsten Scheyer (PIMUZ), Rabea Lilich (SMA), Ben Pabst (SMF/SMA), Andrea Oettl (SMF) and Joep Schaeffer (SMNS) for providing access to their respective collections, as well as for insightful discussions. Christopher Griffin (Princeton University) is thanked for discussions and access to specimen photographs, Jens N. Lallensack (Universidade Federal de Minas Gerais) is thanked for access to specimen photographs and 3D models, and Georg Oleschinski (University of Bonn) for specimen photography. Special thanks go to the Fa. Lücking in Bonenburg, represented by Johannes Thater, to the Wiemers family for their long-standing support of the excavation in Bonenburg and to citizen scientist Michael Mertens for his many years of trusted collaboration. We also wish to express our gratitude to Olaf Dülfer (University of Bonn), as well as to Michael Ludorf, Jerome Gores (both WMNM), and the numerous students and excavation assistants for their valuable contributions in the field and the preparation of the fossils. Finally, we want to thank two anonymous reviewers for their constructive comments that helped us to substantially improve the quality of this manuscript.

References

Barrett, P.M., Chapelle, K.E.J., Sciscio, L., Broderick, T.J., Zondo, M., Munyikwa, D., & Choiniere, J.N. 2024: A new Late Triassic sauropodomorph dinosaur from the Mid-Zambezi Basin, Zimbabwe. – *Acta Palaeontologica Polonica* 69: 227–241. https://doi.org/10.4202/app.01100.2023

Barta, D.E., Nesbitt, S.J. & Norell, M.A. 2018: The evolution of the manus of early theropod dinosaurs is characterized by high inter- and intraspecific variation. – *Journal of Anatomy* 232: 80–104. doi: 10.1111/joa.12719. https://doi.org/10.1111/joa.12719

Benton, M.J., Juul, L., Storrs, G.W. & Galton, P.M. 2000: Anatomy and systematics of the prosauropod dinosaur *Thecodontosaurus antiquus* from the Upper Triassic of southwest England. – *Journal of Vertebrate Paleontology* 20: 77–108. https://doi.org/10.1671/0272-4634(2000)020[0077:AASOTP]2.0.CO;2

Birn-Jeffery, A.V., Miller, C.E., Naish, D., Rayfield, E.J. & Hone, D.W.E. 2012. Pedal claw curvature in birds, lizards and mesozoic dinosaurs – complicated categories and compensating for mass-specific and phylogenetic control. – *PLoS ONE* 7: e50555. https://doi.org/10.1371/journal.pone.0050555

Bonaparte, J.F. 1969: Dos nuevas „faunas" de reptiles triásicos de Argentina. – La estratigrafía del Gondwana, Coloquio de la UICG, Buenos Aires, Argentina, 1–15 de octubre de 1967, Unesco, Paris 1969, 283–306.

Bonaparte, J.F. & Vince, M. 1979: El hallazgo del primer nido de dinosaurios triasicos, (Saurischia, Prosauropoda), Triásico superior de Patagonia, Argentina. – *Ameghiniana* 16: 173–182.

Bonhomme, V. & Claude, J. 2022: Momocs: Morphometrics using R. – R package version 1.4.0. https://cran.r-project.org/package=Momocs

Bonhomme, V., Picq, S., Gaucherel, C. & Claude, J. 2014: Momocs: Outline Analysis Using R. – *Journal of Statistical Software* 56: 1–24. https://doi.org/10.18637/jss.v056.i13

Buckland, W. 1829: XI.--On the discovery of a new species of pterodactyle in the Lias at Lyme Regis. – *Transactions of the Geological Society of London* 2–3: 217–222. https://doi.org/10.1144/transgslb.3.1.217

Camp, C.L. 1936: A new type of small bipedal dinosaur from

the Navajo Sandstone of Arizona. – *University of California Publications, Bulletin of the Department of Geological Sciences* 24: 39–56.

Carrano, M.T., Hutchinson, J.R. & Sampson, S.D. 2005: New information on *Segisaurus halli*, a small theropod dinosaur from the Early Jurassic of Arizona. – *Journal of Vertebrate Paleontology* 25: 835–849. https://doi.org/10.1671/0272-4634(2005)025[0835:NIOSHA]2.0.CO;2

Chapelle, K.E., Barrett, P.M., Botha, J. & Choiniere, J.N. 2019: *Ngwevu intloko*: a new early sauropodomorph dinosaur from the Lower Jurassic Elliot Formation of South Africa and comments on cranial ontogeny in *Massospondylus carinatus*. – *PeerJ* 7: e7240. https://doi.org/10.7717/peerj.7240

Colbert, E.H. 1989: The Triassic dinosaur Coelophysis. – *Bulletin of the Museum of Northern Arizona* 57: 1–174.

Cope, E.D. 1869: Protocol of the March 9, 1869 meeting. – *Proceedings of the Academy of Natural Sciences of Philadelphia* 1869: 316–323.

Cope, E.D. 1889: On a new genus of Triassic Dinosauria. – *The American Naturalist* 23: 626.

Crompton, A.W. & Charig, A.J. 1962: A new ornithischian from the Upper Triassic of South Africa. – *Nature* 196: 1074–1077. https://doi.org/10.1038/1961074a0

Cross, S.R.R., Ivanovski, N., Duffin, C.J., Hildebrandt, C., Parker, A. & Benton, M.J. 2018: Microvertebrates from the basal Rhaetian Bone Bed (latest Triassic) at Aust Cliff, S.W. England. – *Proceedings of the Geologists' Association* 129: 635–653. https://doi.org/10.1016/j.pgeola.2018.06.002

Dalla Vecchia, F.M. 1995: A new pterosaur (Reptilia, Pterosauria) from the Norian (Late Triassic) of Friuli (Northeastern Italy), Preliminary note. – *Gortania* 16: 59–66.

Dalla Vecchia, F.M. 2003: New morphological observations on Triassic pterosaurs. – *Geological Society, London, Special Publications* 217: 23–44. https://doi.org/10.1144/GSL.SP.2003.217.01.03

Dalla Vecchia, F.M. 2009a: Anatomy and systematics of the pterosaur *Carniadactylus* gen. n. *rosenfeldi* (Dalla Vecchia, 1995). – *Rivista Italiana di Paleontologia e Stratigrafia* 115: 159–188. https://doi.org/10.13130/2039-4942/6377

Dalla Vecchia, F.M. 2009b: The first italian specimen of *Austriadactylus cristatus* (Diapsida, Pterosauria) from the Norian (Upper Triassic) of the Carnic Prealps. – *Rivista Italiana di Paleontologia e Stratigrafia* 115: 291–304. https://doi.org/10.13130/2039-4942/6385

Dalla Vecchia, F.M. 2018: Comments on Triassic pterosaurs with a commentary on the "ontogenetic stages" of Kellner (2015) and the validity of B*ergamodactylus wildi*. – *Rivista Italiana di Paleontologia e Stratigrafia* 124: 317–341. https://doi.org/10.13130/2039-4942/10099

Dalla Vecchia, F.M. 2019: *Seazzadactylus venieri* gen. et sp. nov., a new pterosaur (Diapsida: Pterosauria) from the Upper Triassic (Norian) of northeastern Italy. – *PeerJ* 7: e7363. https://doi.org/10.7717/peerj.7363

Dalla Vecchia, F.M. 2021: A revision of the anatomy of the Triassic pterosaur *Austriadraco dallavechiai* Kellner, 2015 and of its diagnosis. – *Rivista Italiana di Paleontologia e Stratigrafia* 127: 427–452. https://doi.org/10.13130/2039-4942/15849

Dalla Vecchia, F.M., Wild, R., Hopf, H. & Reitner, J. 2002: A crested rhamphorhynchoid pterosaur from the Late Triassic of Austria. – *Journal of Vertebrate Paleontology* 22: 196–199.

D'Amore, D.C., Clulow, S., Doody, J.S., Rhind, D. & McHenry, C.R. 2018: Claw morphometrics in monitor lizards: Variable substrate and habitat use correlate to shape diversity within a predator guild. – *Ecology and Evolution* 8: 6766–6778. https://doi.org/10.1002/ece3.4185

Etienne, J.L., Smith, R.E., Unwin, D.M., Smyth, R.S.H. & Martill, D.M. 2024: A 'giant' pterodactyloid pterosaur from the British Jurassic. – *Proceedings of the Geologists' Association* 135: 335–348. https://doi.org/10.1016/j.pgeola.2024.05.002

Eugénio Fernandes, A. 2024: The Pterosauria of the Early to Late Jurassic: contributions to the understanding of the origin and global radiation of the Monofenestrata. – Dissertation, LMU München: Faculty of Geosciences. https://doi.org/10.5282/edoc.34558

Fraas, E. 1913: Die neuesten Dinosaurierfunde in der schwäbischen Trias. – *Naturwissenschaften* 1: 1097–1100. https://doi.org/10.1007/BF01493265

Galton, P.M. 1971: Manus movements of the coelurosaurian dinosaur *Syntarsus* and opposability of the theropod hallux. – *Arnoldia Rhodesia* 5: 1–8.

Galton, P.M. 1973: On the anatomy and relationships of *Efraasia diagnostica* (HUENE) n. gen., a prosauropod dinosaur (Reptilia: Saurischia) from the Upper Triassic of Germany. – *Paläontologische Zeitschrift* 47: 229–255. https://doi.org/10.1007/BF02985709

Galton, P.M. 2014: Notes on the postcranial anatomy of the heterodontosaurid dinosaur *Heterodontosaurus tucki*, a basal ornithischian from the Lower Jurassic of South Africa. – *Revue de Paléobiologie* 33: 97–141.

Galton, P.M. & Van Heerden, J. 1985: Partial hindlimb of *Blikanasaurus cromptoni* n. gen. and n. sp., representing a new family of prosauropod dinosaurs from the upper Triassic of South Africa. – *Geobios* 18: 509–516. https://doi.org/10.1016/S0016-6995(85)80003-6

Galton, P.M. & Van Heerden, J. 1998: Anatomy of the prosauropod dinosaur *Blikanasaurus cromptoni* (Upper Triassic, South Africa), with notes on other tetrapods from the lower Elliot Formation. – *Paläontologische Zeitschrift* 72: 163–177. https://doi.org/10.1007/BF02987824

Galton, P.M. & Kermack, D. 2010: The anatomy of *Pantydraco caducus*, a very basal sauropodomorph dinosaur from the Rhaetian (Upper Triassic) of South Wales, UK. – *Revue de Paléobiologie* 29: 341–404.

Galton, P.M. & Upchurch, P. 2004: Prosauropoda. In: Weishampel, D.B., Dodson, P. & Osmólska, H. (eds), *The Dinosauria*, 232–258. University of California Press, Berkeley, Los Angeles, London.

Galton, P.M., Yates, A.M. & Kermack, D. 2007: *Pantydraco* n. gen. for *Thecodontosaurus caducus* Yates, 2003, a basal sauropodomorph dinosaur from the Upper Triassic or Lower Jurassic of South Wales, UK. – *Neues Jahrbuch für Geologie und Paläontologie, Abhandlungen* 243: 119–125. https://dx.doi.org/10.1127/0077-7749/2007/0243-0119

Gauthier, J. 1986: Saurischian monophyly and the origin of birds. *Memoirs of the California Academy of Sciences* 8: 1–55.

Gravendyck, J., Schobben, M., Bachelier, J.B. & Kürschner, W.M. 2020: Macroecological patterns of the terrestrial vegetation history during the end-Triassic biotic crisis in the central European Basin: A palynological study of the Bonenburg section (NW-Germany) and its supra-regional implications. – *Global and Planetary Change* 194: 103286. https://doi.org/10.1016/j.gloplacha.2020.103286

Hahn, G., Wild, R., & Wouters, G. 1987: Cynodontier-Zähne aus der Ober-Trias von Gaume (S-Belgien). – *Mémoires pour*

servir à l´Explication des Cartes Géologiques et Minières de la Belgique 24: 1–33.

Hartung, J., Sander, P.M., Friedman, M. & Wintrich, T. 2021: First record of mawsoniid coelacanths (Actinistia, Sarcopterygii) from the marine Rhaetian (Upper Triassic) of Bonenburg, Germany. – *Journal of Vertebrate Paleontology* 41: e1931258. https://doi.org/10.1080/02724634.2021.1931258

Hedrick, B.P., Cordero, S.A., Zanno, L.E., Noto, C. & Dodson, P. 2019: Quantifying shape and ecology in avian pedal claws: The relationship between the bony core and keratinous sheath. – *Ecology and Evolution* 9: 11545–11556. https://doi.org/10.1002/ece3.5507

Huene, F. von 1908: Die Dinosaurier der europäischen Triasformation mit Berücksichtigung der außereuröpäischen Vorkommnisse. Jena: G. Fischer.

Huene, F. von 1926: Vollständige Osteologie eines Plateosauriden aus dem schwäbischen Keuper. – *Geologische und Paläontologische Abhandlungen* 15: 1–43.

Huene, F. von 1932: Die fossile Reptil-Ordnung Saurischia, ihre Entwicklung und Geschichte. – *Monographien zur Geologie und Paläontologie* 4: 1–361.

Huene, F. von 1934: Ein neuer Coelurosaurier in der thüringischen Trias. – *Paläontologische Zeitschrift* 16: 145–170.

Inkscape Project 2020: Inkscape. https://inkscape.org

Jagielska, N., O'Sullivan, M., Funston, G.F., Butler, I.B., Challands, T.J., Clark, N.D.L., Fraser, N.C., Penny, A., Ross, D.A., Wilkinson, M. & Brusatte, S.L. 2022: A skeleton from the Middle Jurassic of Scotland illuminates an earlier origin of large pterosaurs. – *Current Biology* 32: 1446–1453. https://doi.org/10.1016/j.cub.2022.01.073

Kaup, J. 1834: Versuch einer Einteilung der Säugetiere in 6 Stämme und der Amphibien in 6 Ordnungen. – *Isis* 3: 311–315.

Kellner, A.W.A. 2015: Comments on Triassic pterosaurs with discussion about ontogeny and description of new taxa. – *Anais da Academica Brasileira Ciências* 87: 669–689. https://doi.org/10.1590/0001-3765201520150307

Konietzko-Meier, D., Werner, J.D., Wintrich, T. & Sander, P.M. 2019: A large temnospondyl humerus from the Rhaetian (Late Triassic) of Bonenburg (Westphalia, Germany) and its implications for temnospondyl extinction. – *Journal of Iberian Geology* 45: 287–300. https://doi.org/10.1007/s41513-018-0092-0

Krebs, B. 1965: *Ticinosuchus ferox* nov. gen. nov. sp. ein neuer Pseudosuchier aus der Trias des Monte San Giorgio. – *Schweizerische paläontologische Abhandlungen* 81: 1–140.

Lautenschlager, S. 2014: Morphological and functional diversity in therizinosaur claws and the implications for theropod claw evolution. – *Proceedings of the Royal Society B: Biological Sciences* 281: 20140497. https://doi.org/10.1098/rspb.2014.0497

Lü, J. 2009: A New Non-Pterodactyloid Pterosaur from Qinglong County, Hebei Province of China. – *Acta Geologica Sinica* (English Edition) 83: 189–199. https://doi.org/10.1111/j.1755-6724.2009.00062.x

Lü, J. & Bo, X. 2011: A New Rhamphorhynchid Pterosaur (Pterosauria) from the Middle Jurassic Tiaojishan Formation of Western Liaoning, China. – *Acta Geologica Sinica* 85: 977–983. https://doi.org/10.1111/j.1755-6724.2011.00531.x

Lü, J., Unwin, D.M., Jin, X., Liu, Y. & Ji, Q. 2010: Evidence for modular evolution in a long-tailed pterosaur with a pterodactyloid skull. – *Proceedings of the Royal Society B: Biological Sciences* 277: 383–389. https://doi.org/10.1098/rspb.2009.1603

Mallison, H. 2010: The digital *Plateosaurus* I: body mass, mass distribution, and posture assessed using CAD and CAE on a digitally mounted complete skeleton. – *Palaeontologia Electronica* 13: 8A.

Marsh, A.D. & Rowe, T.B. 2020: A comprehensive anatomical and phylogenetic evaluation of *Dilophosaurus wetherilli* (Dinosauria, Theropoda) with descriptions of new specimens from the Kayenta Formation of northern Arizona. – *Journal of Paleontology* 94: 1–103. https://doi.org/10.1017/jpa.2020.14

Martill, D.M., Vidovic, S.U., Howells, C. & Nudds, J.R. 2016: The oldest Jurassic dinosaur: A basal neotheropod from the Hettangian of Great Britain. – *PLoS ONE* 11: e0145713. https://doi.org/10.1371/journal.pone.0154352

Meyer, C.E.H. von 1847: *Homeosaurus maximiliani* und *Rhamphorhynchus* (*Pterodactylus*) *longicaudus*, zwei fossile Reptilien aus dem Kalkschiefer von Solenhofen. Frankfurt (Schmerber), p. 22.

Nau, D., Lallensack, J.N., Bachmann, U. & Sander, P.M. 2020: Postcranial osteology of the first early-stage juvenile skeleton of *Plateosaurus trossingensis* from the Norian of Frick, Switzerland. – *Acta Palaeontologica Polonica* 65: 679–708. https://doi.org/10.4202/app.00757.2020

Nesbitt, S.J., Smith, N.D., Irmis, R.B., Turner, A.H., Downs, A. & Norell, M. A. 2009: A complete skeleton of a Late Triassic saurischian and the early evolution of dinosaurs. – *Science* 326: 1530–1533. https://doi.org/10.1126/science.1180350

Novas, F.E. 1993: New information on the systematics and postcranial skeleton of *Herrerasaurus ischigualastensis* (Theropoda: Herrerasauridae) from the Ischigualasto Formation (Upper Triassic) of Argentina. – *Journal of Vertebrate Paleontology* 13: 400–423. https://doi.org/10.1080/02724634.1994.10011523

Novas, F.E., Borges Ribeiro, L.C. & Souza Carvalho, I. de 2005: Maniraptoran theropod ungual from the Marília Formation (Upper Cretaceous), Brazil. – *Revista del Museo Argentino de Ciencias Naturales* nueva serie 7: 31–36. https://doi.org/10.22179/REVMACN.7.344

Osborn, H. F. 1903: On the primary division of the Reptilia into two sub-classes, Synapsida and Diapsida. – *Science* 17: 275–276. https://doi.org/10.1126/science.17.424.275-b

Ostrom, J.H. 1969: Osteology of *Deinonychus antirrhopus*, an unusual theropod from the Lower Cretaceous of Montana. – *Peabody Museum of Natural History, Bulletin* 30: 1–165.

Otero, A. & Pol, D. 2013: Postcranial anatomy and phylogenetic relationships of Mussaurus patagonicus (Dinosauria, Sauropodomorpha). – Journal of Vertebrate Paleontology 33: 1138–1168. https://doi.org/10.1080/02724634.2013.769444

Owen, R. 1842: Report on british fossil reptiles. Part II. – *Report of the British Association for the Advancement of Science 1841:* 60–204.

Owen, R. 1854: Descriptive catalogue of the fossil organic remains of Reptilia and Pisces contained in the Museum of the Royal College of Surgeons of England. London: Taylor and Francis.

Padian, K. 1983: A functional analysis of flying and walking in pterosaurs. – Paleobiology 9: 218–239. https://doi.org/10.1017/S009483730000765X

Perillo, M. & Sander, P.M. 2024: The dinosaurs that weren't: osteohistology supports giant ichthyosaur affinity of

enigmatic large bone segments from the European Rhaetian. – *PeerJ* 12: e17060. https://doi.org/10.7717/peerj.17060

Piechowski, R. & Tałanda M. 2019: The locomotor musculature and posture of the early dinosauriform *Silesaurus opolensis* provides a new look into the evolution of Dinosauromorpha. – *Journal of Anatomy* 236: 1044–1100. https://doi.org/10.1111/joa.13155

Pol, D. & Powell, J.E. 2007: New information on *Lessemsaurus sauropoides* (Dinosauria: Sauropodomorpha) from the upper Triassic of Argentina. – *Special Papers in Palaeontology* 77: 223.

Prino, A., Witzmann, F., Schwermann, A.H., Sander, P.M., Garbay, L. & Konietzko-Meier, D. 2024: How not to disappear completely: new Stereospondyli fossils from the Rhaetian, Upper Triassic of Bonenburg, North Rhine-Westphalia and their implications for the Late Triassic extinction of Stereospondyli. – *Acta Palaeontologica Polonica* 69: 687–712. https://doi.org/10.4202/app.01147.2024

Quinn, J.G., Matheau-Raven, E.R., Whiteside, D.I., Marshall, J.E.A., Hutchinson, D.J. & Benton, M.J. 2024: The relationships and paleoecology of *Pachystropheus rhaeticus*, an enigmatic latest Triassic marine reptile (Diapsida: Thalattosauria). – *Journal of Vertebrate Paleontology*: e2350408. https://doi.org/10.1080/02724634.2024.2350408

R Core Team. 2024: R: A Language and Environment for Statistical Computing. – R Foundation for Statistical Computing, Vienna, Austria. https://www.R-project.org

Raath, M.A. 1969: A new coelurosaurian dinosaur from the Forest Sandstone of Rhodesia. – *Arnoldia (Rhodesia)* 4: 1–254.

Rauhut, O.W.M., Holwerda, F.M. & Furrer, H. 2020: A derived sauropodiform dinosaur and other sauropodomorph material from the Late Triassic of Canton Schaffhausen, Switzerland. – *Swiss Journal of Geosciences* 113: 8. https://doi.org/10.1186/s00015-020-00360-8

Regalado Fernández, O.R. & Werneburg, I. 2022: A new massopodan sauropodomorph from Trossingen Formation (Germany) hidden as 'Plateosaurus' for 100 years in the historical Tübingen collection. – *Vertebrate Zoology* 72: 771–822. https://doi.org/10.3897/vz.72.e86348

Reig, O.A. 1963: La presencia de dinosaurios saurisquios en los „Estratos de Ischigualasto" (Mesotriásico Superior) de las provincias de San Juan y La Rioja (República Argentina). – *Ameghiniana* 3: 3–20.

Renesto, S. 1994: The shoulder girdle and anterior limb of Drepanosaurus unguicaudatus (Reptilia, Neodiapsida) from the Upper Triassic (Norian) of Northern Italy. – *Zoological Journal of the Linnean Society* 111: 247–264. https://doi.org/10.1111/j.1096-3642.1994.tb01485.x

Riley, H. & Stutchbury, S. 1836: A description of various fossil remains of three distinct saurian animals discovered in the autumn of 1834, in the Magnesian Conglomerate on Durdham Down, near Bristol. – *Proceedings of the Geological Society of London* 2: 397–399.

Ripley, B., Venables, B., Bates, D.M., Hornik, K., Gebhardt, A. & Firth, D. 2022: MASS: Support Functions and Datasets for Venables and Ripley's MASS. – R package version 7.3.61. https://cran.r-project.org/package=MASS

Sander, P.M. 1992: The Norian Plateosaurus bonebeds of central Europe and their taphonomy. – *Palaeogeography, Palaeoclimatology, Palaeoecology* 93: 255–299.

Sander, P.M. & Klein, N. 2005: Developmental plasticity in the life history of a prosauropod dinosaur. – *Science* 310 (5755): 1800–1802. https://doi.org/10.1126/science.1120125

Sander, P.M. & Wellnitz, P.W. 2024: A phytosaur osteoderm from a late middle Rhaetian bone bed of Bonenburg (North Rhine-Westphalia, Germany): Implications for phytosaur extinction. – *Fossil Record* 27: 147–158. https://doi.org/10.3897/fr.27.e114601

Sander, P.M., Wintrich, T., Kindlimann, R., Schwermann, A.H. & Kaplan, U. 2016: Die paläontologische Grabung in der Rhät-Lias-Tongrube der Fa. Lücking bei Warburg Bonenburg (Kr. Höxter) im Frühjahr 2015. – *Geologie und Paläontologie in Westfalen 88*: 11–37.

Sander, P.M., Gravendyck, J., Hack, J., Hartung, J., Heijne, J., Kindlimann, R., Konietzko-Meier, D., Lamsfuß, T., Nau, D., Perillo, M., Prino, A., Schaaf, T. & Schwermann, A.H. 2026: Late middle Rhaetian vertebrates from Exter Formation bone beds of Bonenburg (Westphalia, Germany): implications for the end-Triassic extinction event. – Geologie und Paläontologie in Westfalen 99: 23–68.

Sangster, S. 2021: The osteology of *Dimorphodon macronyx*, a non-pterodactyloid Pterosaur from the Lower Jurassic of Dorset, England. – *Monographs of the Palaeontographical Society* 175: 1–48. https://doi.org/10.1080/02693445.2021.2037868

Schaeffer, J. 2024: Osteological redescription of the holotype of *Plateosaurus trossingensis* (Dinosauria: Sauropodomorpha) from the Upper Triassic of SW Germany and its phylogenetic implications. – *Journal of Systematic Palaeontology* 22: 2335387. https://doi.org/10.1080/14772019.2024.2335387

Schwermann, A.H. 2016: Über den Nachweis von *Lepagia gaumensis* (Eucynodonta incertae sedis) aus dem Rhät (Trias) von Warburg-Bonenburg (Kr. Höxter). – *Geologie und Paläontologie in Westfalen 88*: 35–44.

Schwermann, A.H., Wintrich, T. & Sander, P.M. 2017: Das Ende der Trias–paläontologische Grabung im Rhät von Warburg-Bonenburg. – *Archäologie in Westfalen-Lippe*: 23–25. https://doi.org/10.11588/aiw.2017.0.57662

Sereno, P.C. 1993: The pectoral girdle and the forelimb of the basal theropod *Herrerasaurus ischigualastensis*. – *Journal of Vertebrate Paleontology* 13: 425–450. https://doi.org/10.1080/02724634.1994.10011524

Sereno, P.C. 2012: Taxonomy, morphology, masticatory function and phylogeny of heterodontosaurid dinosaurs. – *Zookeys* 226: 1–225. https://doi.org/10.3897/zookeys.223.2840

Slater, T.S., Duffin, C.J., Hildebrandt, C., Davies, T.G. & Benton, M.J. 2016: Microvertebrates from multiple bone beds in the Rhaetian of the M4–M5 motorway junction, South Gloucestershire, U.K. – *Proceedings of the Geologists' Association* 127: 464–477. https://doi.org/10.1016/j.pgeola.2016.07.001

Stecher, R. 2008: A new Triassic pterosaur from Switzerland (Central Austroalpine, Grisons), *Raeticodactylus filisurensis* gen. et sp. nov. – *Swiss Journal of Geosciences* 101: 185–201. https://doi.org/10.1007/s00015-008-1252-6

Swift, A. & Martill, D.M. 1999: Fossils of the Rhaetian Penarth Group. – *Palaeontological Association Field Guides to Fossils 9*: 1–312.

Theodori, C. 1830: Knochen vom *Pterodactylus* aus der Liasformation von Banz. – *Notizen aus dem Gebiete der Natur- und Heilkunde 29*: 101–103.

Thomson, T.J. & Motani, R. 2021: Functional morphology of vertebrate claws investigated using functionally based categories and multiple morphological metrics. – *Journal*

of Morphology 282: 449–471. https://doi.org/10.1002/jmor.21317

Tinius, A. & Russell, A.P. 2017: Points on the curve: An analysis of methods for assessing the shape of vertebrate claws. – *Journal of Morphology* 278: 150–169. https://doi.org/10.1002/jmor.20625

Unwin, D.M. 1996: The fossil record of Middle Jurassic pterosaurs. In: Morales, M. (ed.), *The Continental Jurassic*, 291–304. Museum of Northern Arizona, USA.

Van Heerden, J. & Galton, P. 1997: The affinities of *Melanorosaurus* – A Late Triassic prosauropod dinosaur from South Africa. – *Neues Jahrbuch für Geologie und Paläontologie Monatshefte* 1997: 39–55. https://doi.org/10.1127/njgpm/1997/1997/39

Venables, W.N. & Ripley, B.D. 2002: *Modern Applied Statistics with S.* – Springer, New York. https://doi.org/10.1007/978-0-387-21706-2

Wang, X., Kellner, A.W.A., Jiang, S., Meng, X. 2009: An unusual long-tailed pterosaur with elongated neck from western Liaoning of China. – *Anais da Academia Brasileira de Ciências* 81: 793–812. https://doi.org/10.1590/S0001-37652009000400016

Wang, X., Kellner, A.W.A., Jiang, S., Cheng, X., Meng, X. & Rodrigues, T. 2010: New long-tailed pterosaurs (Wukongopteridae) from western Liaoning, China. – *Anais da Academia Brasileira de Ciências* 82: 1045–1062. https://doi.org/10.1590/S0001-37652010000400024

Wang, X., Zhou, Z., Zhang, F. & Xu, X. 2002: A nearly completely articulated rhamphorhynchoid pterosaur with exceptionally well-preserved wing membranes and ?hairs? from Inner Mongolia, northeast China. – *Chinese Science Bulletin* 47: 226–230. https://doi.org/10.1360/02tb9054

Welles, S.P. 1970: *Dilophosaurus* (Reptilia: Saurischia), a new name for a dinosaur. – *Journal of Paleontology* 44: 989.

Welles, S.P. 1984: *Dilophosaurus wetherilli* (Dinosauria, Theropoda): osteology and comparisons. – *Palaeontographica Abteilung A* 185: 85–180.

Wild, R. 1978: Die Flugsaurier (Reptilia, Pterosauria) aus der Oberen Trias von Cene bei Bergamo, Italien. – *Estratto dal Bollettino della Società Paleontologica Italiana* 17: 176–256.

Wild, R. 1984: Flugsaurier aus der Obertrias von Italien. – *Naturwissenschaften* 71: 1–11. https://doi.org/10.1007/BF00365973

Wintrich, T., Hayashi, S., Houssaye, A., Nakajima, Y. & Sander, P.M. 2017: A Triassic plesiosaurian skeleton and bone histology inform on evolution of a unique body plan. – *Science Advances* 3: e1701144. https://doi.org/10.1126/sciadv.1701144

Witton, M.P. 2013: *Pterosaurs: Natural History, Evolution, Anatomy*. – Princeton University Press.

Yates, A.M., Bonnan, M.F., Neveling, J., Chinsamy, A. & Blackbeard, M.G. 2010: A new transitional sauropodomorph dinosaur from the Early Jurassic of South Africa and the evolution of sauropod feeding and quadrupedalism. – *Proceedings of the Royal Society of London B: Biological Sciences* 277: 787–794. https://doi.org/10.1098/rspb.2009.1440

You, H.-L., Azuma, Y., Wang, T., Wang, Y.-M. & Dong, Z.-M. 2014: The first well preserved coelophysoid theropod dinosaur from Asia. – *Zootaxa* 3873: 233–249. https://doi.org/10.11646/zootaxa.3873.3.3

Young, C.-C. 1941: A complete osteology of *Lufengosaurus huenei* Young (gen. et sp. nov.). – *Palaeontologia Sinica, Series C* 7: 1–53.

Zahner, M. & Brinkmann, W. 2019: A Triassic averostranline theropod from Switzerland and the early evolution of dinosaurs. – *Nature Ecology & Evolution* 3: 1146–1152. https://doi.org/10.1038/s41559-019-0941-z

Zambelli, R. 1973: *Eudimorphodon ranzii* gen. nov., sp. nov. uno pterosauro triassico. – *Rendiconti Instituto Lombardo Accademia* 107: 27–32.

Editor: Manja Hethke